JCTC Journal of Chemical Theory and Computation

# Solvent Dependence of $^{14}$N Nuclear Magnetic Resonance Chemical Shielding Constants as a Test of the Accuracy of the Computed Polarization of Solute Electron Densities by the Solvent

Raphael F. Ribeiro, Aleksandr V. Marenich, Christopher J. Cramer,* and Donald G. Truhlar*

*Department of Chemistry and Supercomputing Institute, University of Minnesota, 207 Pleasant Street SE, Minneapolis, Minnesota 55455-0431*

Received May 20, 2009

**Abstract:** Although continuum solvation models have now been shown to provide good quantitative accuracy for calculating free energies of solvation, questions remain about the accuracy of the perturbed solute electron densities and properties computed from them. Here we examine those questions by applying the SM8, SM8AD, SMD, and IEF-PCM continuum solvation models in combination with the M06-L density functional to compute the $^{14}$N magnetic resonance nuclear shieldings of $CH_3CN$, $CH_3NO_2$, $CH_3NCS$, and $CH_3ONO_2$ in multiple solvents, and we analyze the dependence of the chemical shifts on solvent dielectric constant. We examine the dependence of the computed chemical shifts on the definition of the molecular cavity (both united-atom models and models based on superposed individual atomic spheres) and three kinds of treatments of the electrostatics, namely the generalized Born approximation with the Coulomb field approximation, the generalized Born model with asymmetric descreening, and models based on approximate numerical solution schemes for the nonhomogeneous Poisson equation. Our most systematic analyses are based on the computation of relative $^{14}$N chemical shifts in a series of solvents, and we compare calculated shielding constants relative to those in $CCl_4$ for various solvation models and density functionals. While differences in the overall results are found to be reasonably small for different solvation models and functionals, the SM*x* models SM8, and SM8AD, using the same cavity definitions (which for these models means the same atomic radii) as those employed for the calculation of free energies of solvation, exhibit the best agreement with experiment for every functional tested. This suggests that in addition to predicting accurate free energies of solvation, the SM8 and SM8AD generalized Born models also describe the solute polarization in a manner reasonably consistent with experimental $^{14}$N nuclear magnetic resonance spectroscopy. Models based on the nonhomogeneous Poisson equation show slightly reduced accuracy. Scaling the intrinsic Coulomb radii to larger values (as has sometimes been suggested in the past) does not uniformly improve the results for any kind of solvent model; furthermore it uniformly degrades the results for generalized Born models. Use of a basis set that increases the outlying charge diminishes the accuracy of continuum models that solve the nonhomogeneous Poisson equation, which we ascribe to the inability of the numerical schemes for approximately solving the nonhomogeneous Poisson equation to fully account for the effects of electronic charge outside the solute cavity.

## 1. Introduction

Nuclear magnetic resonance (NMR) shielding parameters are very sensitive to the molecular electronic structure,[1−3] and for molecules in solution they can serve as a probe of the solute response to intermolecular interactions. Buckingham et al.[4] proposed a rationalization of solvent effects on chemical shifts by separating these effects into four contributions: (i) bulk magnetic susceptibility of the medium, (ii) anisotropy in the molecular magnetic susceptibility of the solvent, (iii) van der Waals forces, and (iv) polar interactions, which were considered to include hydrogen bonds. The

* Corresponding author e-mails: cramer@umn.edu (C.J.C.); truhlar@unm.edu (D.G.T.).

10.1021/ct900258f CCC: $40.75 
Published on Web 07/30/2009

Kamlet-Taft system of solvent properties[5,6] approaches the problem of solvent shifts and shielding parameters in a different way by considering the shielding parameter in cyclohexane as a reference and adding four different contributions for other solvents related to (i) the hydrogen-bond donor strength of the solvent, (ii) the solvent hydrogen-bond acceptor character, (iii) solvent polarizability, and (iv) a correction for superpolarizability of aromatic and highly chlorinated solvents.

Nitrogen shielding has received a great deal of attention in the study of solvent shifts since the lone pair on nitrogen often leads to particularly large shifts in electron density in response to an environment.[7−14] For this reason, several attempts were made to rationalize a broad range of experimental results for this nucleus, and a variety of schemes have been used for the computation of the solvent influence on nitrogen NMR shielding parameters.[7−12,15−26] These methods differ quantitatively in the way that the various contributions mentioned above are taken into account.

Modeling the solvent as a continuum has proven to be useful in predicting free energies of solvation provided that the solvent is characterized not only by the bulk dielectric constant but also by solvent and solute-dependent interfacial surface tensions that account for cavitation, dispersion, and local changes to solvent structure such as hydrogen bonds to the solute, solute disruption of the bulk-solvent hydrogen bonding network, and local changes to the solvent dielectric constant, especially in the first solvent shell.[27−34] However, the partition of free energies of solvation into bulk electrostatics effects and interfacial effects is not unique.[35] Since the former effects are usually[36,37] included by a self-consistent reaction field (SCRF), which affects the solute electronic density and properties, but the latter are usually treated post-SCF, which neglects their effects on the solute wave function or density and hence on solute properties, the success of a model for free energies of solvation does not guarantee its success for properties such as nuclear shieldings in solution. Nevertheless, it is disappointing that approaches based on continuum solvation models tested so far do not consistently explain many of the experimental results for nitrogen chemical shifts in different solvents, even though sometimes the trends are correct. To understand this situation better, the present study evaluates the performance of the newest models of the SM*x* series of solvation models (SM8,[31] SM8AD,[34] and SMD[33]) for solvent shifts and compares the results to those obtained with continuum solvent models[38−44] present in popular quantum chemistry codes[45,46] and with the work of Zhan and Chipman[16] in order to evaluate their absolute ability and relative ability to account for this response property and to ascertain whether any of the parametrization methods or electrostatic treatments that have been employed are systematically better than any of the others.

In section 2 we describe the test sets. Relevant theoretical background is summarized in section 3, while section 4 gives computational details, and section 5 provides the methodologies employed. Sections 6 and 7 contain results and discussion, and section 8 summarizes the main conclusions.

## 2. Test Sets

In the current article we compare and discuss nuclear shielding changes due to solvent-to-solvent transfer. In principle, theory could also be tested for gas-to-solvent shifts, but there are larger uncertainties associated with experimental measurements of these quantities, and they also pose a substantially greater challenge to the underlying electronic structure theory, which obscures the testing of solvation models. Thus we assess the performance of solvation models only for solvent-to-solvent shifts. Specifically, we restrict ourselves to well-established experimental results for acetonitrile ($CH_3CN$),[9] nitromethane ($CH_3NO_2$),[7] methyl nitrate ($CH_3ONO_2$),[8] and methyl isothiocyanate ($CH_3NCS$)[8] in a range of solvents. These four solutes are characterized by diverse nitrogen functional groups for which $^{14}$N chemical shifts have been measured in multiple solvents with external neat nitromethane as a reference. Corrections for bulk solvent magnetic susceptibility were made[7−9] in the acquisition of the experimental data.

## 3. Theory

**3.A. Solvation Models.** Continuum solvation models represent a solvated molecule at an atomic level of detail inside a molecule-sized electrostatic cavity surrounded by a dielectric medium that represents the solvent. In some older work the cavity was a sphere, but here, as in most modern work, the cavity is solute-shaped and either is a superposition of atomic spheres with empirical radii or is a superposition of united atoms (a nonhydrogenic atom and its attached hydrogens), again with sizes defined by empirical parameters. In the electrostatic theory of dielectric media, the medium has associated with it a relative permittivity $\varepsilon$, which is a scalar function of position for isotropic nonhomogeneous media. Following the convention most popular in the chemical literature, $\varepsilon$ will be called the dielectric constant. The charge distribution of the solute (charge density) induces polarization in the surrounding dielectric medium, and the self-consistently determined interaction between the solute charge distribution and the electric polarization field of the solvent, when adjusted for the energetic cost of polarizing the solute and the solvent, constitutes what is called the electrostatic contribution to the free energy of solvation. More properly, when one makes the usual assumption that the dielectric constant in regions containing solvent is given by the bulk value and then neglects the difference of the local dielectric constant in the near-solute region from its bulk value, this should be called the bulk-electrostatic contribution. The electric potential due to the polarized dielectric continuum and the polarization of the solute equals the total potential minus the electrostatic potential[47] of the gas-phase solute molecule. The total electric potential satisfies the nonhomogeneous Poisson equation (NPE) for electrostatics

$$\nabla \cdot (\varepsilon \nabla \Phi) = -4\pi\rho_f \qquad (1)$$

where $\rho_f$ is the solute charge density, and the word "nonhomogeneous" refers to the specification of the dielectric constant as different inside the solute cavity (where it is given the value unity) and in the solvent region (where it is given

the bulk value). Therefore, the reaction field can be obtained self-consistently by numerical integration of the NPE coupled to the quantum mechanical electron density of the solute molecule. From the reaction field one calculates the free energy change corresponding to the solvation process. The bulk-electrostatic contribution to the free energy of solvation is given by[48]

$$\Delta G_{\mathrm{EP}} = \left\langle \Psi | H^{(0)} - \frac{e}{2}\phi | \Psi \right\rangle + \frac{e}{2}\sum_k Z_k \phi_k - \langle \Psi^{(0)} | H^{(0)} | \Psi^{(0)} \rangle \tag{2}$$

where $e$ is the atomic unit of charge, $\phi_k$ is the reaction field evaluated at atom $k$, $Z_k$ is the atomic number of atom $k$, $H^{(0)}$ and $\Psi^{(0)}$ are the solute electronic Hamiltonian and electronic wave function, respectively, in the gas phase, and $\Psi$ is the polarized solute electronic wave function in solution. This equation includes the polarization of the solvent by the solute and the distortion of the solute that is induced by this polarization effect. Note that when one uses density functional theory, there is no wave function so the wave function appearing in eq 2 is replaced by the Kohn−Sham determinant of the noninteracting reference system, and the Hamiltonian operator is replaced by the appropriate density functional analog.

NPE solvers that employ the continuous charge density (without approximating it by distributed point charges or multipoles) are called density-based solvation models. Other implicit solvation models solve the NPE using alternative representations of the continuous density, for example, single- or multicenter multipolar expansions. An alternative continuum model, the generalized Born (GB) approximation,[27,49−56] does not start with the NPE but instead employs a starting point based on Coulomb's law and represents the solute as a collection of point charges (a distributed monopole approximation), located at the nuclear positions.

In the present study, we employ six solvation models. Four of them are based on the Integral-Equation-Formalism[39,40,42] of the Polarizable Continuum Model[38] (IEF-PCM) algorithm for solving the NPE using the polarized continuous quantum mechanical charge density of the solute. The first of these, called the SMD[33] model (SM is a general prefix for solvation models developed in our group, and "D" in the name stands for "density"), and the other three IEF-PCM-based models[38,41,43,45] differ in the atomic radii used to define the boundary between solute and solvent. The other two models are Solvation Model 8 (SM8)[31] and Solvation Model 8 with Asymmetric Descreening (SM8AD),[34] both of which utilize the GB approximation for bulk electrostatics based on self-consistently polarized class IV[57] partial atomic charges. In most of the calculations here we use the CM4M charge model,[58] although these models can also be employed with a more general CM4[30] charge model.

We can now revisit a key issue already raised in the Introduction. In all the SM$x$ models employed here ($x$ = D, 8, or 8AD), the observable fixed-concentration solvation free energy is partitioned algorithmically into two components. The first component is the bulk electrostatic contribution resulting from the interaction of a solute with its reaction field, which is the electric field produced by the polarized charge density that the solute induces in the solvent. This component is treated self-consistently. The second component is called the cavity-dispersion-solvent-structure (CDS) term and is the contribution arising from short-range interactions between the solute and solvent molecules in the first solvation shell. This contribution is a sum of terms that are proportional (with geometry-dependent proportionality constants called atomic surface tensions) to the solvent-accessible surface areas of the individual atoms of the solute.[27−34,54,55] In all SM$x$ models, the CDS term is not included in the self-consistent reaction field procedure, and, therefore, it does not alter the resulting electronic wave function and it has no effect on system properties (such as dipole moments or NMR chemical shifts) other than the free energy of solvation. The other widely available parametrizations based on PCM[37,41,43,45] also involve non-bulk-electrostatic terms (usually called cavity-dispersion-repulsion terms) that do not influence the calculation of solute properties (note that "non-bulk-electrostatic" means terms that are not due to bulk electrostatics, not electrostatic terms that are nonbulk in character). Thus, we will consider only the bulk-electrostatic problem hereafter.

A key issue in all implicit solvation models is the boundary between the solute cavity where $\varepsilon < \varepsilon_s$ and the solvent continuum where $\varepsilon = \varepsilon_s$. In the SMD, SM8, and SM8AD models, or in PCM models employing scaled Bondi[59] radii (see below), the boundary between the solute cavity and the solvent dielectric continuum is defined to enclose a superposition of nuclear-centered spheres with radii $\rho_{z_k}$, which are called intrinsic Coulomb radii. The intrinsic Coulomb radii depend only on the atomic numbers $Z_k$ of the atoms. This boundary forms a so-called solvent-accessible surface (SAS). The IEF-PCM-based calculations use the following approximation of the reaction field at an arbitrary position $\mathbf{r}$ within the SAS

$$\phi(\mathbf{r}) = \sum_m \frac{q_m}{|\mathbf{r} - \mathbf{r}_m|} \tag{3}$$

where $\mathbf{r}_m$ is the position of the center of an element $m$ of surface area on the solute−solvent boundary (such elements are called tessarae), and $q_m$ is an apparent surface charge on element $m$. In contrast, the GB approximation within the SM8 and SM8AD protocols is equivalent to approximating the reaction field distribution as

$$\phi_k = \sum_{k'} \frac{q_{k'}}{|\mathbf{r}_k - \mathbf{r}_{k'}|} f_{kk'} \tag{4}$$

where $\mathbf{r}_k$ and $\mathbf{r}_{k'}$ are evaluated only at atomic positions, $q_{k'}$ is a partial charge on atom $k'$, and $f_{kk'}$ is a function to be specified. The value of a single term in eq 4 is called a Coulomb integral.

One successful function $f_{kk'}$ for approximating the Coulomb integrals is the dielectric descreening approximation of Still et al.,[53] which yields

$$f_{kk'} = -\left(1 - \frac{1}{\varepsilon_s}\right) \frac{r_{kk'}}{\sqrt{r_{kk'}^2 + \alpha_k \alpha_{k'} \exp(-r_{kk'}^2/d\alpha_k\alpha_{k'})}} \tag{5}$$

where

$$r_{kk'} \equiv |\mathbf{r}_k - \mathbf{r}_{k'}| \tag{6}$$

and where $d$ is a parameter, $\varepsilon_s$ is the dielectric constant of the bulk solvent, and $\alpha_k$ is the descreened atomic radius of atom $k$; $\alpha_k$ represents an appropriately weighted average distance of atom $k$ from the solvent, and it is called a Born radius. The number of elements $m$ in eq 3 is in principle increased to convergence, whereas the number of terms $k'$ in eq 4 is equal to the number of atoms in the solute. A relation connecting eqs 3−6 is given as follows[37]

$$\sum_m q_m = -\left(1 - \frac{1}{\varepsilon_s}\right)\sum_{k'} q_{k'} \tag{7}$$

The SM8 model treats dielectric descreening effects by the Coulomb-field approximation[53] such that a partial effective charge in the solute interacts with the solvent by a charge-induced dipole interaction that varies as $r^{-4}$, where $r$ is the distance between the partial atomic charge and a volume element of the continuum solvent. The Coulomb-field approximation leads to the following formula for the Born radius[53−55]

$$\alpha_k = \left(\frac{1}{R'} + \int_{\rho_{Z_k}}^{R'} \frac{A_k(r)}{4\pi r^4}\,\mathrm{d}r\right)^{-1} \tag{8}$$

In eq 8, $R'$ is the radius of the sphere centered on atom $k$ that completely engulfs all other spheres centered on the other atoms of the solute, $\rho_{Z_k}$ is the intrinsic Coulomb radius of atom $k$, and $A_k(r)$ is the exposed area of a sphere of radius $r$ that is centered on atom $k$. This area depends on the geometry of the solute and the radii of the spheres centered on all the other atoms in the solute.

Grycuk has shown recently[56] that, when the partial atomic charge is asymmetrically situated in the molecule, i.e., not located at the center of the molecule, one can apparently estimate the dielectric descreening more accurately by using a shorter-range function proportional to $r^{-6}$. Therefore the SM8AD model uses an alternative functional form for the Born radius $\alpha_k$, which is given by[56]

$$\alpha_k = \left(\frac{1}{R'^3} + \int_{\rho_{Z_k}}^{R'} \frac{3A_k(r)}{4\pi r^6}\mathrm{d}r\right)^{-1/3} \tag{9}$$

The SM8AD model is an extension of the SM8 model that replaces eq 8 by eq 9 to better account for the asymmetric descreening (AD).

SM8, SMD, and SM8AD have atomic radii optimized to free energies of solvation for ions. The four PCM-based models we consider are SMD and three older models whose bulk electrostatic treatment differs from SMD only in the choice of the solute−solvent boundary: (i) PCM-UA0, where UA0 is a united atom topological model;[44] (ii) PCM-UAKS, which also uses united atoms,[41] but in this case optimized for the calculation of free energies of solvation with Kohn−Sham density functional theory;[45] (iii) and PCM-1.2B where 1.2B denotes that the cavities are based on atomic spheres defined by Bondi's atomic radii times 1.2. The Bondi radii[59] are widely used atomic van der Waals radii, and the scale factor used here is 1.2, which, plus or minus ∼0.05, is a widely used value adopted by several groups.[37,60−64] The PCM-UA0 and PCM-1.2B models are effectively defined for all solvents because the only solvent-dependent parameter upon which there is a non-negligible dependence of the electrostatic response is $\varepsilon$. However, the electrostatic response of the UAKS model depends significantly not only on $\varepsilon$ but also on $\alpha$, which is a scale factor for solute radii. For the solvents considered in this article, $\alpha$ is 1.4 for cyclohexane, benzene, carbon tetrachloride, chloroform, dichloromethane, acetone, acetonitrile, and dimethylsulfoxide, 1.3 for diethyl ether, and 1.2 for ethanol, methanol, and water; and it is undefined for hexane, 1,4-dioxane, 2,2,2-trifluoro-ethanol, *N,N*-dimethylformamide, and ethylene glycol. We note that changing $\alpha$ from 1.2 to 1.4 can have a large effect on the chemical shift, often as much as 2−3 ppm.

We will also compare to some calculations of Zhan and Chipman[16] so it is useful to place their methods and nomenclature in the context of what was discussed above. Zhan and Chipman point out that the usual approximate solutions of the NPE in terms of an apparent polarization charge density on the cavity surface are valid only when the solute charge is entirely within the surface, which is never the case for real solutes because all atomic and molecular wave functions have exponentially decreasing tails. For real solutes, one also needs to introduce an apparent polarization charge density in the volume outside the cavity. Zhan and Chipman use SPE to denote methods that neglect this and SVPE to denote methods that include it. Chipman also points out that one can simulate volume polarization by adding additional apparent surface charge density,[25,65,66] and he calls this SS(V)PE.[25] Although a simple surface-polarization NPE solver would correspond to the SPE approach,[25] the IEF-PCM model includes an implicit correction for the effect of solute charge outside the cavity, and it can be formulated so as to be exactly the same as SS(V)PE.[37]

**3.B. Nuclear Magnetic Resonance Chemical Shielding.** NMR shielding constant tensors are calculated using a variational perturbative approach.[67−69] For a nucleus $K$ they are calculated by

$$\sigma_k = 1 + \left.\frac{\partial^2 G(B,I)}{\partial I_k \partial B}\right|_{B=0,I_k=0} \tag{10}$$

where $I_k$ is the nuclear magnetic moment, $B$ is the magnitude of the applied magnetic field, and $G$ is the free energy of the system. For the gauge invariance of the origin problem,[67] the most popular approach is to work with gauge invariant atomic orbitals (GIAO),[70−72] which includes complex factors in the basis functions and gives rise to gauge-invariant molecular properties. Other common methods to deal with this issue in quantum chemistry codes include Individual Gauge for Localized Orbitals (IGLO)[73] and Continuous Set of Gauge Transformations (CSGT)[74] (which is equivalent to the CTOCD-DZ scheme of Lazzeretti[75,76]).

The chemical shift is defined as minus the difference between the nuclear shielding constant and a reference value.

## 4. Computational Details

**4.A. Software.** All the calculations in this study were done using a locally modified version[77,78] of the *Gaussian03*[45] electronic structure suite.

**4.B. DFT/M06-L.** For our electronic structure model we chose to use density functional theory (DFT) and in particular the meta-GGA local functional M06-L.[79] We based this choice on a recent study[80] indicating that M06-L predicted NMR chemical shielding constants the most accurately in a comparison of several modern functionals for a diverse data set.

**4.C. CSGT.** The Continuous Set of Gauge Transformations[74] method was used in this work to calculate shielding constants, since the more popular GIAO[70−72] approach is not implemented in *Gaussian03* for meta-GGA or hybrid meta-GGA density functionals. Cheeseman et al.[81] have shown that CSGT and GIAO give very similar results, except that CSGT seems to have a slower convergence with respect to basis set.

**4.D. Basis Set and Geometries.** It is known that calculations of NMR chemical shielding tensors are very sensitive to basis set size and quality. However, it is also recognized that there is no reliable population analysis based on calculations that employ large basis sets.[82] Therefore, the CM4 and CM4M charge models, used to compute $q_k$ values in the SM8 and SM8AD solvation models, do not have parameters for triple-$\zeta$ or larger basis sets. To learn more about basis set requirements, various exploratory studies were carried out. In section 6.A we present the influence of basis sets on the chemical shift of acetonitrile in four different solvents. Section 6.D.3 gives a different perspective by analyzing the effects of using a large basis set including diffuse functions and a smaller basis set with all core functions decontracted, in the computations of relative nitrogen shielding constants for the whole set of experimental data used in this work.

Since there is disagreement in the literature[16,19,24,83,84] concerning the influence of geometry relaxation effects on solvent shifts, we similarly studied acetonitrile in four different solvents with and without solution-phase geometry optimization. These results are in section 6.B.

## 5. Methods

**5.A. Fitting Approach.** In the first part of this study, we followed an approach similar to one taken by Zhan and Chipman[16] to uniformly shift the calculated results so as best to compare with the experimental data in solution and in particular with the *change* in chemical shift as a function of solvent. The convention adopted here is the one in which the positive direction of the scale corresponds to increasing magnetic shielding (upfield).

The first step taken was to calculate the nitrogen isotropic chemical shielding for the four selected solutes in four or five arbitrary solvents by SM8, SMD, and SM8AD. Since all of the experimental data used were relative to external neat nitromethane, we uniformly shifted the calculated results by a constant amount in order to correct, in a least-squares sense, for this and systematic errors (e.g., basis set incompleteness, approximate density functional, etc.). For each solvation model and solute, a shifting constant labeled $D$ was obtained. The new values of relative shielding constants ($\sigma_{calc} + D$) were then fit to the following equation

$$\sigma = B + A/\varepsilon \tag{11}$$

where $\sigma$ is equal to the calculated shielding $\sigma_{calc} + D$, $B$ and $A$ are optimized parameters, and $\varepsilon$ is the dielectric constant of the medium. If $\sigma$ were a function only of the dielectric constant, and if only polarization effects were important, $B + A$ could be regarded as the gas phase value, but since that is not true we cannot guarantee any physical meaning to them.

The parameters $A$ and $B$ were separately fit for each solute and method. An equation describing the dielectric dependence of each solute for each of the SM$x$ models was found, and the results were plotted as a function of $(\varepsilon\text{-}1)/\varepsilon$. The same procedure was applied for each of the models with intrinsic Coulomb radii scaled by 0.8 and 1.2 to gauge the sensitivity of the results to these parameters and because scaling the radii by different factors had previously been determined sometimes to give improved results in prior studies with different solvation models.[16,21,22]

Since the wave function of the solute is affected only by bulk electrostatic effects in the solvation models used here, $A$ and $B$ reflect only polarization contributions to the solvent shift. Other specific contributions such as the high anisotropy of molecular magnetizability in some solvents such as benzene,[4] van der Waals forces, and the deviation of hydrogen bonding from a purely electrostatic effect would be implicitly included in the parameters $A$ and $B$ were the fitting procedure of eq 11 to be applied to experimental data as opposed to the theoretical data derived from the continuum solvation models. Our goals here are to determine the degree to which the three SM$x$ models predict the correct variation of the shielding constants compared to experiment, to examine more closely those cases where they fail, to identify possible corrections in such cases, and to see in general how the predicted results are affected by scaling the intrinsic Coulomb radii.

**5.B. Solvent Shifts Relative to $CCl_4$.** Based on the results obtained with the method described in section 5.A, we formulated an extended approach to compute $^{14}N$ solvent shifts vs carbon tetrachloride as a reference solvent. In particular, for solutes where the nitrogen atom is likely to be involved in hydrogen bonds as an acceptor and the solvent has an Abraham's hydrogen bond acidity[85] $\alpha \geq 0.5$ (note that our $\alpha$ is called $\sum\alpha_2$ by Abraham), we suggest calculations with liquid-phase optimized solute−solvent clusters to improve accuracy. A complete discussion of this approach with results for the SM$x$ models, a comparison with other implicit solvation methods, and the effects of scaling the radii by an increasing factor are presented in section 6.D.

## 6. Results and Discussion

We use SMD in sections 6.A and 6.B, SMD, SM8, and SM8AD in section 6.C, and all six solvation models in section 6.D. Experimentalists interested only in the solvent

***Table 1.*** Calculated Relative $^{14}$N Shielding Constants (in ppm) of Acetonitrile with Gas-Phase Geometry Optimized by M06-L/6-311++G(2df,2p)

| solvent shift | 6-31G(d) | 6-31+G(d,p) | 6-311++G(3df,3p) | aug-pcS-3 |
|---|---|---|---|---|
| cyclohexane-water | 12.8 | 14.0 | 16.2 | 16.6 |
| cyclohexane-acetone | 11.6 | 12.7 | 14.7 | 15.0 |
| cyclohexane-chloroform | 7.0 | 7.6 | 8.7 | 9.0 |
| chloroform-water | 5.8 | 6.4 | 7.4 | 7.6 |
| chloroform-acetone | 4.7 | 5.1 | 5.9 | 6.1 |
| acetone-water | 1.2 | 1.3 | 1.5 | 1.5 |

shifts on NMR shielding constants may skip sections 6.A−6.C and go straight to 6.D.

**6.A. Basis Set Dependence of Nuclear Shielding.** Since we are concerned with solvent shifts, an exploratory study was done to examine the effect of basis sets on this relative quantity. We selected acetonitrile as the solute, with the gas-phase geometry optimized by M06-L/6-311++G(2df,2p), and we calculated the nitrogen shielding constants using SMD as the solvent model in four different solvents, namely: cyclohexane, chloroform, water, and acetone, with each of the following basis sets: 6-31G(d), 6-31+G(d,p), 6-311++G-(3df,3p),[86−90] and the quadruple-$\zeta$ aug-pcS-3,[91−93] which was specially designed for the computation of nuclear magnetic resonance shielding constants by density functional methods.

The results are presented in Table 1; the largest differences between the solvent-to-solvent shifts calculated with aug-pcS-3 and 6-31G(d) are 3.78 and 3.42 ppm, but the ordering of the solvent-to-solvent shifts is consistent between the two basis sets. Since 6-31G(d) has well-established CM4M parameters, which are necessary for the computation of $q_k$ values in eq 4, we decided to use this basis set for all chemical shift calculations, unless stated otherwise.

Irrespective of the convenience of the 6-31G(d) basis set for use with the SM8 and SM8AD models, the choice of this smaller basis set may also be more accurate for the SMD and PCM calculations, in spite of the usual rule that "bigger is better" when it comes to basis sets for electronic structure calculations. In particular we note that Zhan and Chipman[16] compared the performance of an SPE continuum solvation model (which is defined in section 3.A) that employs a surface-charge formalism to represent the solvent reaction to solute charge inside the cavity to that of an SVPE model that also includes polarization due to solute charge in the volume external to the molecular cavity. They observed that the former led to inaccurate chemical shift variations unless unrealistically large cavities were employed, while a "normal" cavity (defined as one that could also be put to routine use for computing free energies of solvation) was able to give realistic results only when volume polarization was included.[16] This problem should be mitigated in the SMD and PCM models examined in this article because they are all based on IEF-PCM, which (as discussed in section 3.A) should be able to simulate volume polarization. Nevertheless this observation suggests that the use of larger basis sets, particularly those that include diffuse functions that permit additional electronic charge density outside a typical solute cavity, may lead to instability in SMD-based and PCM-based chemical shift calculations. In contrast, decontracting the core basis functions centered on the atoms present in the system cannot lead to increased charge penetration, as the portion of the electronic density described by these functions is certainly inside the molecular cavity. Therefore, this approach should give improved chemical shifts. We will assess these points further in section 6.D.3.

***Table 2.*** Relative Shielding Constants (in ppm) of Acetonitrile Calculated Using the Gas-Phase and Liquid-Phase Geometries

| solvent shift | liquid geometry | gaseous geometry |
|---|---|---|
| cyclohexane-water | 13.1 | 12.8 |
| cyclohexane-acetone | 11.9 | 11.6 |
| cyclohexane-chloroform | 7.1 | 7.0 |
| chloroform-water | 5.9 | 5.8 |
| chloroform-acetone | 4.8 | 4.7 |
| acetone-water | 1.2 | 1.2 |

**6.B. Geometry Relaxation Effects.** In order to decide whether or not to optimize the geometry of the solute in the liquid phase, we carried out an exploratory study to look at geometry relaxation effects on the chemical shift. We selected acetonitrile as our test solute because it has the largest range of solvent-to-solvent shifts (23 ppm) of the four solutes in the test set.[7−9] Acetonitrile was optimized in cyclohexane, water, acetone, and chloroform at the SMD/M06-L/6-311++G(2df,2p) level, and the NMR shielding constants were calculated in each solvent at the SMD/M06-L level but with the 6-31G(d) basis set. The trends shown in Table 2 make it clear that optimizing the geometry in the different liquids has little quantitative effect on the solvent-to-solvent shifts. Therefore, all the geometries used here were optimized at the gas phase M06-L/6-311++G(2df,2p) level, unless mentioned otherwise.

**6.C. Dependence of the Chemical Shift on Dielectric Constant.** *6.C.1. Solvent Shifts of Acetonitrile.* $^{14}$N chemical shift data have been reported[9] for acetonitrile in fourteen solvents with neat nitromethane as an external reference. Table 3 and Figure 1 compare computed and experimental results. Each curve describing the dielectric dependence of the $CH_3CN$ $^{14}$N chemical shift (using eq 11) was fitted to the computed isotropic shielding constants in $CCl_4$ ($\varepsilon$ = 2.2280), $CH_2Cl_2$ ($\varepsilon$ = 8.93), $CH_3CN$ ($\varepsilon$ = 35.688), and $CHCl_3$ ($\varepsilon$ = 4.7113).[94] We show here only the plots for standard models. Plots for models having scaled radii are presented in the Supporting Information. Mean unsigned errors between theory and experiment were calculated using the following equation

$$\mathrm{MUE} = \sum_{i=1}^{N} \frac{|\sigma_i - \sigma_{\mathrm{exp},i}|}{N} \qquad (12)$$

***Table 3.*** Fitting Parameters of Eq *11* and MUEs (ppm) for $^{14}$N Chemical Shifts of Acetonitrile

| | *D* | *B* | *A* | MUE | MUEX[b] |
|---|---|---|---|---|---|
| | | | $F = 1$[a] | | |
| SM8 | 86.09 | 136.97 | −20.31 | 3.4 | 2.2 |
| SMD | 83.35 | 139.53 | −25.92 | 3.5 | 2.7 |
| SM8AD | 89.10 | 135.96 | −15.26 | 3.4 | 2.1 |
| | | | $F = 0.8$ | | |
| SM8 | 75.02 | 141.18 | −41.29 | 4.6 | 4.2 |
| SMD | 71.85 | 142.54 | −48.10 | 6.1 | 5.3 |
| SM8AD | 81.34 | 138.74 | −29.12 | 5.3 | 2.6 |
| | | | $F = 1.2$ | | |
| SM8 | 91.02 | 135.33 | −12.11 | 3.5 | 2.1 |
| SMD | 89.21 | 136.22 | −16.53 | 3.3 | 2.0 |
| SM8AD | 92.94 | 134.75 | −9.21 | 3.7 | 2.3 |

[a] *F* is a scaling factor for the intrinsic Coulomb radii in each of the models, where unity corresponds to the standard models. [b] Mean unsigned errors excluding the solvents water and TFE.

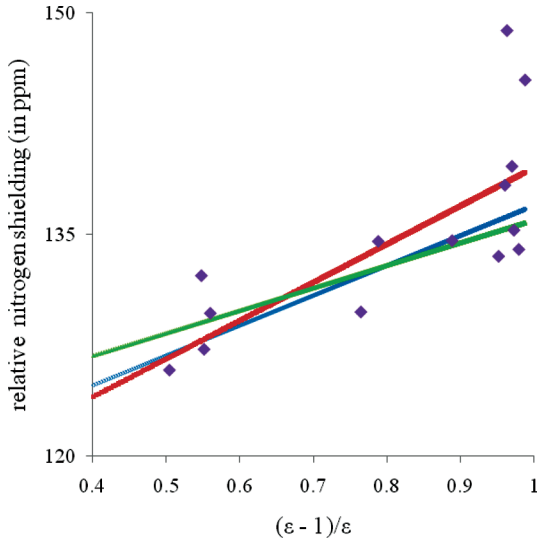


***Figure 1.*** Acetonitrile nitrogen shielding as a function of solvent dielectric constant. Diamonds represent experimental results, the red curve represents eq 11 fitted to SMD results, the blue curve represents eq 11 fitted to SM8 results, and the green curve represents eq 11 fitted to SM8AD results.

where $\sigma_i$ refers to the value predicted by eq 11 for a solvent having dielectric constant $\varepsilon$, $\sigma_{exp}$ is the experimental value,[9] and *N* is the number of experimental results for a given molecule.

Table 3 indicates that scaling the standard intrinsic Coulomb radii of the SM8 and SM8AD models either fails to improve the predicted results or improves them by at most a very small amount. For SMD, on the other hand, increasing the radii by a factor of 1.2 does show an improvement in the MUE. The SM*x* models show correct qualitative dielectric dependence of the $^{14}$N chemical shielding in solute acetonitrile. There are, however, large discrepancies between the experimental and computed results for water and 2,2,2-trifluoroethanol (TFE). Both of these solvents are strong hydrogen bond donors, and it seems reasonable to assume that hydrogen bonding to the nitrile nitrogen lone pair may be responsible for this disagreement. Thus, the MUEs for acetonitrile were also calculated excluding water and TFE (last column of Table 3), resulting in an error reduction from

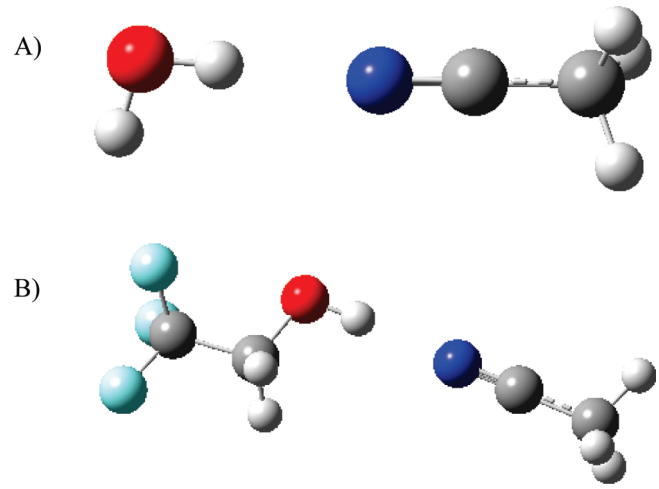


***Figure 2.*** Liquid-phase optimized solute−solvent clusters for A) acetonitrile-water and B) acetonitrile-2,2,2-trifluoroethanol.

***Table 4.*** Acetonitrile $^{14}$N Shielding Constants (ppm) in Water and TFE Relative to $CCl_4$ as Solvent

| solvent | SM8 | SMD | SM8AD | experiment |
|---|---|---|---|---|
| | | Cluster of Acetonitrile with Solvent | | |
| water | 14.1 | 15.7 | 13.3 | 18.2 |
| 2,2,2-trifluoroethanol | 17.4 | 18.3 | 17.5 | 21.6 |
| | | Only Implicit Solvent | | |
| water | 8.1 | 11.1 | 5.9 | 18.2 |
| 2,2,2-trifluoroethanol | 7.5 | 11.0 | 5.5 | 21.6 |

34% to 39% for the models with standard radii. For water and TFE, a correction in the calculated shifts to account for hydrogen bonding is discussed in the next section.

If we exclude water and TFE, SM8AD delivers the best performance for solvent-to-solvent shifts in the case of acetonitrile using standard radii. SM8 is nearly as accurate, and SMD is the most accurate of all if the cavity radii are scaled by a factor of 1.2.

*6.C.2. Cluster Calculations of Hydrogen-Bonding Corrections to the Solvent Shift.* The data for $CH_3CN$ suggest that hydrogen bonds play a role in nuclear shielding that is not well described by continuum solvation models. To evaluate this point further, we optimized acetonitrile-water and acetonitrile-TFE clusters in their respective liquid phases at the SM8/M06-L/6-31G(d) level and the shielding constants were calculated for the clusters with each of the SM*x* models using the 6-31G(d) basis set. Figure 2 shows the geometries of the optimized clusters in solution, and Table 4 presents the results of this approach compared to the fully implicit solvent case.

The fully implicit solvent approach significantly underestimates the shieldings and also predicts higher shielding constants for water than for TFE, which fails to agree with the experimental data. The cluster calculations are in significantly improved agreement with experiment and also give the correct order for water vs TFE. SMD is the model that is most quantitatively accurate here, but SM8 and SM8AD also indicate the importance of clustering.

*6.C.3. Solvent Shifts of Methyl Isothiocyanate.* Measurements of $^{14}$N chemical shifts in $CH_3NCS$ have been reported

***Table 5.*** Fitting Parameters[a] and MUEs (ppm) for $^{14}$N Shielding Constants of Methyl Isothiocyanate

| | *D* | *B* | *A* | MUE |
|---|---|---|---|---|
| | | $F = 1$[b] | | |
| SM8 | 105.99 | 290.37 | 7.50 | 1.5 |
| SMD | 109.16 | 288.68 | 13.68 | 1.9 |
| SM8AD | 106.60 | 290.01 | 8.79 | 1.6 |
| | | $F = 0.8$ | | |
| SM8 | 106.99 | 289.44 | 10.92 | 1.7 |
| SMD | 113.26 | 286.77 | 21.47 | 2.7 |
| SM8AD | 108.34 | 288.54 | 14.22 | 1.9 |
| | | $F = 1.2$ | | |
| SM8 | 104.88 | 290.99 | 5.20 | 1.5 |
| SMD | 106.60 | 290.04 | 8.68 | 1.6 |
| SM8AD | 105.38 | 290.74 | 6.13 | 1.5 |

[a] Equation 11. [b] $F$ is a scaling factor for the intrinsic Coulomb radii in each of the models, where $F = 1$ corresponds to the standard models.

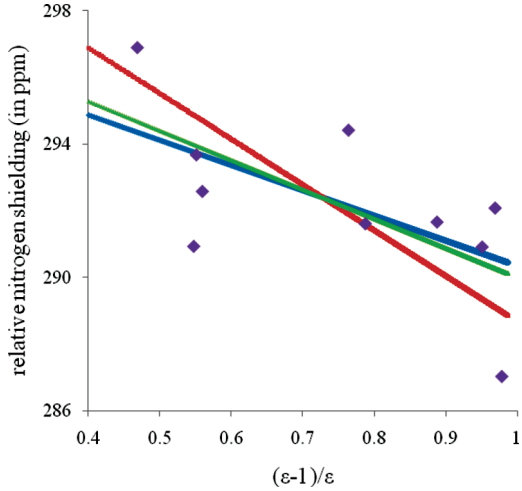


***Figure 3.*** Nitrogen shielding in $CH_3NCS$ as a function of solvent dielectric constant. Diamonds represent experimental results, the red curve represents eq 11 fitted to SMD results, the blue curve represents eq 11 fitted to SM8 results, and the green curve represents eq 11 fitted to SM8AD results.

in ten solvents.[8] The experimental data range over 9.9 ppm. Fits to eq 11 were based on the calculated $^{14}$N data in *n*-hexane ($\varepsilon = 1.8819$), 1,4-dioxane ($\varepsilon = 2.2099$), $CHCl_3$ ($\varepsilon = 4.7113$), $CH_2Cl_2$ ($\varepsilon = 8.93$), and acetone ($\varepsilon = 20.493$).[94] Table 5 and Figure 3 present the results.

Again, scaling the model radii fails to have much effect on the mean accuracy of the SM8 or SM8AD results, but a scaling factor of 1.2 leads to improved accuracy for SMD. The SM*x* models are all consistent with the experimental trend of decreasing chemical shift with increasing dielectric constant. Such behavior contrasts with that of the SPE and SVPE models of Zhan and Chipman,[16] who hypothesized that untreated nonelectrostatic effects were required to capture this trend. The cavities for SPE and SVPE are chosen as surfaces of constant electron density; this is in contrast to the SM*x* models, which use fixed radii for individual atoms. One possible explanation is that in the case of MeNCS, the isodensity surface varies in ways that reverses the inverse relationship between chemical shift and the dielectric function seen here for the constant radius models, and this causes the isodensity models to fail to reproduce the direction of the experimental trend.

***Table 6.*** Fitting Parameters of Eq *11* and MUEs (ppm) for $^{14}$N Chemical Shifts of Methyl Nitrate

| | *D* | *B* | *A* | MUE |
|---|---|---|---|---|
| | | $F = 1$[a] | | |
| SM8 | 89.41 | 38.90 | 4.67 | 0.9 |
| SMD | 89.60 | 38.67 | 5.63 | 0.8 |
| SM8AD | 89.87 | 38.73 | 5.41 | 0.8 |
| | | $F = 0.8$ | | |
| SM8 | 91.17 | 38.18 | 7.83 | 0.6 |
| SMD | 92.09 | 37.64 | 10.22 | 0.7 |
| SM8AD | 91.86 | 37.89 | 9.10 | 0.6 |
| | | $F = 1.2$ | | |
| SM8 | 88.45 | 39.16 | 3.49 | 1.0 |
| SMD | 88.45 | 39.12 | 3.66 | 1.0 |
| SM8AD | 88.57 | 39.19 | 3.38 | 1.0 |

[a] $F$ is a scaling factor for the intrinsic Coulomb radii in each of the models; $F = 1$ corresponds to the standard models.

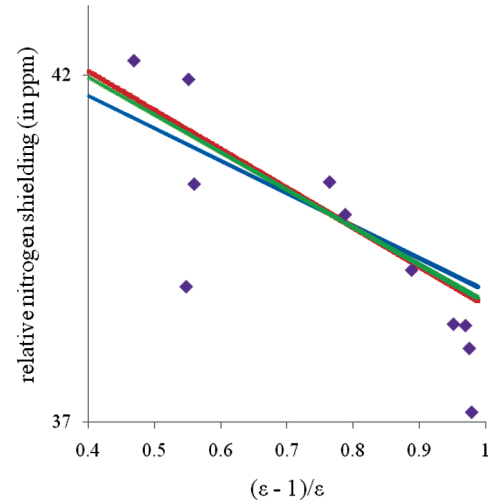


***Figure 4.*** Nitrogen shielding of $CH_3ONO_2$ as a function of solvent dielectric constant. Diamonds represent experimental results, the red curve represents eq 11 fitted to SMD results, the blue curve represents eq 11 fitted to SM8 results, and the green curve represents eq 11 fitted to SM8AD results.

*6.C.4. Solvent Shifts of Methyl Nitrate.* For $CH_3ONO_2$, nitrogen NMR data have been reported in 12 solvents.[8] The experimental data range over only 5.1 ppm, i.e., this solute is the least sensitive to solvent of the four considered here. Fits to eq 11 were based on the calculated $^{14}$N data in *n*-hexane ($\varepsilon = 1.8819$), $CHCl_3$ ($\varepsilon = 4.7113$), $CH_2Cl_2$ ($\varepsilon = 8.93$), and acetone ($\varepsilon = 20.493$).[94] The results found are presented in Table 6 and Figure 4.

The use of radii scaled by a factor of 0.8 leads to improvements in the accuracy of all three SM*x* models, but the sensitivity of the MUEs to radii is rather small, varying by at most about 0.4 ppm over the scaling range from 0.8 to 1.2. We note that the methyl nitrate data set does contain measurements for 1,2-ethanediol and 2,2,2-trifluoroethanol as solvents. However, while these solvents have $\alpha \geq 0.5$, no unusual deviation is observed from the continuum predictions, consistent with the nitrogen atom in the nitrate functional group being a poor hydrogen-bond acceptor.

***Table 7.*** Fitting Parameters and MUEs (ppm) for $^{14}$N Chemical Shifts of Nitromethane

| | *D* | *B* | *A* | MUE |
|---|---|---|---|---|
| | | *F* = 1.0[a] | | |
| SM8 | 79.78 | −0.16 | 13.19 | 1.5 |
| SMD | 78.29 | −0.18 | 13.27 | 1.5 |
| SM8AD | 80.57 | −0.42 | 14.51 | 1.6 |
| | | *F* = 0.8 | | |
| SM8 | 86.32 | −2.39 | 25.01 | 2.3 |
| SMD | 84.68 | −2.38 | 24.91 | 2.3 |
| SM8AD | 87.79 | −2.92 | 27.81 | 2.7 |
| | | *F* = 1.2 | | |
| SM8 | 76.36 | 0.80 | 8.02 | 1.6 |
| SMD | 75.52 | 0.76 | 8.24 | 1.6 |
| SM8AD | 76.58 | 0.74 | 8.34 | 1.6 |

[a] *F* is the scaling factor for the intrinsic Coulomb radii; *D*, *B*, and *A* are defined by eq 11.

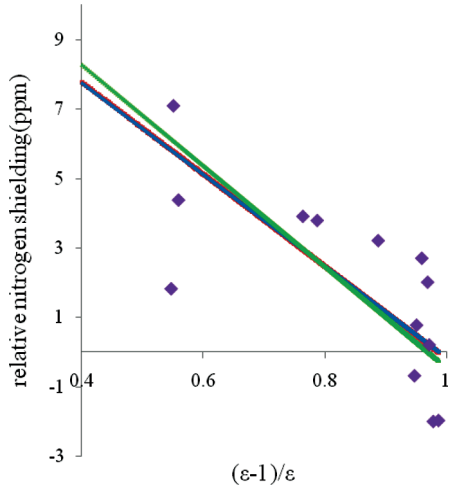


***Figure 5.*** Nitrogen shielding in $CH_3NO_2$ as a function of solvent dielectric constant. Diamonds represent experimental results, the red curve represents eq 11 fitted to SMD results, the blue curve represents eq 11 fitted to SM8 results, and the green curve represents eq 11 fitted to SM8AD results.

*6.C.5. Solvent Shifts of Nitromethane.* For $CH_3NO_2$, NMR experiments have been carried out in thirteen solvents, and the experimental data range over 9.1 ppm.[7] Fits to eq 11 were based on the calculated $^{14}$N data in benzene ($\varepsilon$ = 2.2706), diethyl ether ($\varepsilon$ = 4.24), acetone ($\varepsilon$ = 20.493), and acetonitrile ($\varepsilon$ = 35.688).[94] Table 7 and Figure 5 present the results.

Scaling the cavity radii does not improve the results for any SM*x* model, although scaling by a factor of 1.2 does not degrade the results much either. Considering Figure 5, the discrepancy between experiment and theory is somewhat larger for nitromethane than for the other three solutes studied here, but the largest error is for 1,4-dioxane as solvent (4.1 ppm). The source of this error is not clear, as no particular structural effects associated with this solvent are obvious.

*6.C.6. General Discussion of the Fitting Approach.* Table 8 shows the combined MUE and RMSE for each of the SM*x* models tested, including the models with scaled radii but excluding acetonitrile in water and 2,2,2-trifluoroethanol. For the SM8 and SM8AD models, the best results are obtained with the standard model radii. For the SMD model, a quantitative improvement of about 0.2 ppm is obtained after scaling of the radii by a factor of 1.2. This same scaling decreases the accuracy of the SM8 and SM8AD models by small margins. All of the models exhibit significantly poorer performance when a scale factor of 0.8 is used.

***Table 8.*** MUEs and RMSEs (ppm) for Combined Eq *11* Fits

| | MUE | RMSE |
|---|---|---|
| | *F* = 1.0[a] | |
| SM8 | 1.5 | 1.8 |
| SMD | 1.7 | 2.1 |
| SM8AD | 1.5 | 1.8 |
| | *F* = 0.8 | |
| SM8 | 2.2 | 3.1 |
| SMD | 2.7 | 3.8 |
| SM8AD | 2.0 | 2.6 |
| | *F* = 1.2 | |
| SM8 | 1.5 | 1.9 |
| SMD | 1.5 | 1.8 |
| SM8AD | 1.6 | 2.0 |

[a] *F* is the scaling factor for the intrinsic Coulomb radii.

Zhan and Chipman,[16] in an approach that motivated the one used here, tested their SVPE and SPE solvent models with the molecular cavity being defined by various isodensity contours, and they found in their best case a root mean squared error of 2.3 ppm for 48 experimental data (we have used 49). Table 8 shows that the SM*x* models have somewhat improved quantitative accuracy compared to SVPE and SPE; in particular they have root mean squared errors of only 1.8−2.1 ppm. Furthermore they correctly predict the inverse dependence of the $^{14}$N chemical shift of methyl isothiocyanate on dielectric constant. Zhan and Chipman[16] had concluded that the inclusion of volume polarization is very important for the solvation effects on nitrogen shielding. Therefore it is very encouraging that all three SM*x* methods yield a smaller root mean squared error and exhibit more accurate trends than the SVPE model, which includes this effect. SM8 and SM8AD do not treat volume polarization explicitly, and SMD treats it approximately, like SS(V)PE, because it is based on IEF-PCM.

Mennucci et al. also studied the dependence of nitrogen shielding constants on the cavity size,[21,22] with the concern that cavities that may give qualitatively correct free energies of solvation could lead to inaccurate molecular properties. Various approaches were tested, the most important ones being the following: scaling all the intrinsic Coulomb radii by the same factors, scaling different groups (in the case of a united-atom approach) by different factors, and mixing different kinds of molecular cavities with different scaling factors, i.e., mixing scaled Bondi radii for some atoms with scaled radii for united-atom groups. For acetonitrile in water, they found that scaling the van der Waals radii by 1.4 improved the results in a reasonable manner, while no improvements were seen in the case of cyclohexane.[21] However, in a different paper,[22] an opposite trend was found, since scaling all radii by 1.4 gave rise to improved results for diazines in cyclohexane, but no improvement was seen for water.

Based on these other results and those reported here, it would appear that the radii that have been optimized against free energies of solvation for continuum models that ap-

proximately solve the Poisson equation are somewhat too small for the accurate calculation of $^{14}N$ chemical shifts, as scaling the radii optimized for free energies by factors ranging from 1.2 to 1.4 tends to lead to improved accuracy (although not in every instance). With the generalized Born models, on the other hand, a single set of radii seems equally suited to either task, although scaling the radii by a factor of 1.2 only degrades chemical shift predictions by a small amount. However, these conclusions are based on a fitting approach that may improve the results in a nonsystematic manner. To understand this situation better, another study was performed to more directly investigate the effects of scaling the radii in generalized Born and NPE models, and the results are discussed in section 6.D.2.

**6.D. Solvent Shifts Relative to $CCl_4$.** *6.D.1. Standard Radii.* Equation 11, as used in section 6.C, offers a method to assess the qualitative accuracy of the various solvation models with respect to predicting solvation effects on $^{14}N$ chemical shifts, but, in the absence of data in enough solvents to do a fit, it is not a practical means for actually predicting chemical shift values. In this section we present a more straightforward protocol for the computation of $^{14}N$ solvent-to-solvent shifts. Since this protocol calculates solvent-to-solvent shifts, it is convenient to define a reference solvent. We choose $CCl_4$ as it does not make hydrogen bonds, and it is a commonly used solvent.

In the procedure adopted in this section, one calculates the shielding in a desired solvent using one of the SM*x* models, and one calculates the difference from the result obtained by the same model for the shielding in the reference solvent, $CCl_4$. If the nitrogen atom of the solute for which the solvent shift is being calculated is known to make strong hydrogen bonds with the chosen solvent, then a cluster calculation is carried out with one explicit solvent molecule (and the rest of the solvent still implicit); otherwise all solvent molecules are implicit. The criterion we adopted for deciding if this situation applies to a specific system is whether the Abraham's hydrogen bond acidity of the solvent in which the solute is immersed is greater than 0.5. In this work, this criterion applied only to $CH_3CN$ in water and TFE, and the cluster geometries for these two cases were optimized in the liquid phase with SM8/M06-L/6-31G(d).

In order to place the performance of the SM*x* models in the context of what can be obtained with other implicit solvation models for solvent-to-solvent shifts, we compared three other models to experiment employing the same basis set (6-31G(d)), the same gas-phase M06-L/6-311++G(2df,2p) geometries, and the same liquid-phase SM8/M06-L/6-31G(d) cluster geometries. The implicit models to which we compared are three IEF-PCM continuum solvent methods present in the popular *Gaussian03* computer package: (i) PCM with UA0[44] radii, (ii) PCM with UAKS[41] radii, and (iii) PCM with Bondi's atomic radii[59] multiplied by the scaling factor 1.2. For (i) we computed the solvent shifts using the B3LYP[95−98] and M06-L[79] density functionals. B3LYP was chosen simply because it is the most popular functional in the chemical literature, and UA0 radii were chosen because they are the default option for PCM calculations in *Gaussian03*. In the case of PCM with the UAKS radii (ii), we chose to use M06-L and PBE0[99] as the density functional since the UAKS parameters were optimized for density functional theory with the PBE0/6-31G(d) method. For (iii) we did calculations only with M06-L. SM8AD calculations were also done with B3LYP and PBE0 in order to assess sensitivity to density functional. Results are presented in Tables 9 and 10 for each solute in the order of increasing solvent dielectric constant. In these tables, as well as later tables, mean unsigned errors were computed from unrounded data.

Large deviations are observed when 1,4-dioxane is chosen as a solvent. This solvent evidently gives rise to interactions that cannot be described by any of the implicit solvent models, all of which are restricted to describing results related to changes in dielectric constant. Benzene is another problematic nonpolar solvent, but this is more understandable as the continuum solvent models cannot reproduce effects such as solvent ring current, which may affect the nuclear shielding constants of solute atoms in aromatic solvents. Continuum solvent models also neglect charge transfer between solute and solvent.

The SM*x* models SM8 and SM8AD provide the lowest MUEs compared to experiment for any of the functional/solvation model combinations tested. However, none of the models show particularly large errors, although use of the UA0 radii in conjunction with PCM cannot be recommended. MUEs from SM8AD with B3LYP and PBE0 are about 0.2 ppm better than those with M06-L. The good performance of SM8 relative to PCM-UA0 is particularly interesting since it has been suggested by three of the authors of *Gaussian03* and co-authors[100] that the reason that the UA0 cavities (which are the default choice in *Gaussian03*) predict less accurate free energies of solvation than SM8 is that they represent a compromise designed to give insight into various solute properties, including magnetic properties and response properties. Although the research underlying the mentioned compromise is apparently unpublished, the inference one could draw from that suggestion is that PCM-UA0 might give more accurate magnetic response properties than SM8. The results here indicate that this is not the case. The SM8 model is more accurate, although the SM8 model was clearly optimized only for free energies of solvation. We should note though that there was an attempt to make the model as physical as possible within the constraints of the chosen functional forms (e.g., no specification of types of atoms is used, and the radii are independent of both overall charge and partial atomic charges).

*6.D.2. Solvent Shifts Relative to $CCl_4$ - Scaled Radii Models.* Since the fitting approach indicated that scaling the radii of SMD by a factor of 1.2 improved agreement with experiment, we decided to test this issue for the case of shifts relative to carbon tetrachloride described in section 6.D.1. We examined three models, namely, SMD, PCM-1.2B, and SM8. For each of these models, all of the radii were scaled by a factor of 1.2 (meaning for PCM-1.2B the final radii were 1.44 times larger than Bondi radii), and the nitrogen shielding was calculated with the M06-L functional and 6-31G(d) basis set. The results for these methods are present in Table 11. In no instance is agreement with experiment

***Table 9.*** Predicted Relative Shielding Constants (ppm) Using the M06-L Density Functional

| | SM8 | SMD | SM8AD | PCM-UA0 | PCM-UAKS | PCM-1.2B | experiment |
|---|---|---|---|---|---|---|---|
| | | | | $CH_3CN$ | | | |
| $CCl_4$-$C_6H_{12}$ | −0.8 | −0.1 | −0.7 | −0.9 | −0.6 | −0.9 | −1.4 |
| $CCl_4$-1,4-dioxane | −0.1 | −0.1 | −0.1 | −0.1 | NA[a] | −0.1 | 5.0 |
| $CCl_4$-$C_6H_6$ | 0.1 | 0.1 | 0.1 | 0.1 | 0.0 | 0.1 | 2.4 |
| $CCl_4$-$Et_2O$ | 4.1 | 5.3 | 3.2 | 4.3 | 4.9 | 4.7 | 2.5 |
| $CCl_4$-$CHCl_3$ | 4.4 | 6.0 | 3.3 | 4.9 | 3.5 | 5.4 | 7.3 |
| $CCl_4$-$CH_2Cl_2$ | 6.6 | 8.6 | 5.0 | 7.1 | 5.0 | 7.8 | 7.4 |
| $CCl_4$-acetone | 8.3 | 10.6 | 6.3 | 8.7 | 6.1 | 9.6 | 6.3 |
| $CCl_4$-EtOH | 8.5 | 11.0 | 6.4 | 8.9 | 12.0 | 9.8 | 11.1 |
| $CCl_4$-TFE[b] | 17.4 | 18.3 | 17.5 | 15.8 | NA | 17.2 | 21.6 |
| $CCl_4$-MeOH | 8.7 | 11.2 | 6.6 | 9.2 | 12.3 | 10.1 | 12.4 |
| $CCl_4$-$CH_3CN$ | 8.6 | 11.3 | 6.5 | 9.2 | 6.5 | 10.2 | 8.1 |
| $CCl_4$-DMSO | 9.0 | 11.5 | 6.8 | 9.4 | 6.6 | 10.4 | 6.8 |
| $CCl_4$-water[b] | 14.1 | 15.7 | 13.3 | 12.3 | 15.1 | 14.2 | 18.2 |
| MUE | 2.5 | 2.4 | 2.8 | 2.8 | NA | 2.6 | |
| | | | | $CH_3NO_2$ | | | |
| $CCl_4$-1,4-dioxane | 0.0 | 0.3 | 0.0 | 0.0 | NA | 0.0 | −5.3 |
| $CCl_4$-$C_6H_6$ | −0.1 | 0.2 | −0.1 | 0.0 | −0.0 | 0.0 | −2.7 |
| $CCl_4$-$Et_2O$ | −2.5 | −2.0 | −2.7 | −1.9 | −2.5 | −2.3 | −3.2 |
| $CCl_4$-$CHCl_3$ | −2.8 | −3.3 | −3.1 | −2.2 | −1.7 | −2.6 | −3.3 |
| $CCl_4$-$CH_2Cl_2$ | −4.0 | −4.2 | −4.5 | −3.2 | −2.5 | −3.8 | −3.9 |
| $CCl_4$-acetone | −5.1 | −4.7 | −5.6 | −3.9 | −3.0 | −4.6 | −6.3 |
| $CCl_4$-EtOH | −5.0 | −7.9 | −5.5 | −4.0 | −6.4 | −4.8 | −4.4 |
| $CCl_4$-MeOH | −5.1 | −8.7 | −5.6 | −4.1 | −6.5 | −5.0 | −5.1 |
| $CCl_4$-$CH_3CN$ | −5.6 | −5.3 | −6.1 | −4.1 | −3.2 | −5.0 | −6.9 |
| $CCl_4$-DMF | −5.2 | −4.8 | −5.7 | −4.1 | NA | −5.0 | −7.8 |
| $CCl_4$-DMSO | −5.2 | −4.9 | −5.8 | −4.2 | −3.3 | −5.0 | −9.1 |
| $CCl_4$-$H_2O$ | −8.8 | −9.1 | −9.5 | −4.3 | −6.8 | −5.2 | −9.1 |
| MUE | 1.6 | 2.3 | 1.5 | 2.6 | NA | 2.0 | |
| | | | | $CH_3NCS$ | | | |
| $CCl_4$-$C_6H_{14}$ | 0.5 | 0.9 | 0.6 | 0.7 | NA | 0.6 | 3.2 |
| $CCl_4$-1,4-dioxane | 0.0 | 0.0 | 0.0 | 0.0 | NA | 0.0 | −2.7 |
| $CCl_4$-$C_6H_6$ | −0.1 | 0.0 | −0.1 | 0.0 | 0.0 | −0.1 | −1.1 |
| $CCl_4$-$Et_2O$ | −1.6 | −2.8 | −1.8 | −2.3 | −2.6 | −1.9 | 0.7 |
| $CCl_4$-$CHCl_3$ | −1.6 | −3.2 | −1.8 | −2.6 | −1.9 | −2.3 | −2.1 |
| $CCl_4$-$CH_2Cl_2$ | −2.5 | −4.6 | −2.9 | −3.8 | −2.7 | −3.3 | −2.0 |
| $CCl_4$-acetone | −3.2 | −5.7 | −3.8 | −4.7 | −3.3 | −4.0 | −2.8 |
| $CCl_4$-MeOH | −3.4 | −6.0 | −4.1 | −5.0 | −6.6 | −4.2 | −1.6 |
| $CCl_4$-DMSO | −3.5 | −6.2 | −4.2 | −5.1 | −3.5 | −4.3 | −6.7 |
| MUE | 1.7 | 2.4 | 1.8 | 2.1 | NA | 1.9 | |
| | | | | $CH_3ONO_2$ | | | |
| $CCl_4$-$C_6H_{14}$ | 0.3 | 0.3 | 0.4 | 0.3 | NA | 0.3 | 0.3 |
| $CCl_4$-1,4-dioxane | 0.0 | 0.1 | 0.0 | 0.0 | NA | 0.0 | −3.0 |
| $CCl_4$-$C_6H_6$ | 0.0 | 0.0 | 0.0 | 0.0 | 0.0 | 0.0 | −1.5 |
| $CCl_4$-$Et_2O$ | −0.1 | −1.0 | −1.1 | −0.9 | −1.1 | −1.1 | −1.5 |
| $CCl_4$-$CHCl_3$ | −1.2 | −1.6 | −1.4 | −1.0 | −0.8 | −1.2 | −1.9 |
| $CCl_4$-$CH_2Cl_2$ | −1.7 | −1.7 | −1.9 | −1.5 | −1.1 | −1.7 | −2.7 |
| $CCl_4$-acetone | −1.9 | −1.9 | −2.2 | −1.8 | −1.4 | −2.1 | −3.5 |
| $CCl_4$-TFE | −1.9 | −3.8 | −2.2 | −1.9 | NA | −2.3 | −3.9 |
| $CCl_4$-MeOH | −1.9 | −3.8 | −2.2 | −1.9 | −2.7 | −2.3 | −3.5 |
| $CCl_4$-1,2-ethanediol | −1.9 | −3.9 | −2.3 | −1.9 | NA | −2.3 | −3.9 |
| $CCl_4$-DMSO | −2.0 | −2.3 | −2.3 | −1.9 | −1.5 | −2.3 | −4.8 |
| MUE | 1.5 | 1.0 | 1.3 | 1.6 | NA | 1.4 | |
| subset MUE[c] | 1.6 | 1.9 | 1.6 | 2.0 | 1.9 | 1.7 | |
| total MUE | 1.9 | 2.0 | 1.9 | 2.3 | NA | 2.0 | |

[a] NA denotes not applicable because the method is not defined for this solvent. [b] These results were provided by cluster calculations with the solute and a single solvent molecule optimized with SM8/M06-L/6-31G(d). [c] Includes only the rows where all methods are defined.

improved compared to the results provided in Table 9. While this may in part be associated with choosing carbon tetrachloride as a reference solvent, it suggests that scaling of radii cannot be considered to be a general requirement for accurate NPE-based predictions, and the fitting approach embodied in eq 11 is best employed only to assess qualitatively the dielectric dependence of the solvent shifts predicted by each model.

Another way to scale the radii is to scale them differently in each solvent, as in the UAKS model. The original example of this is the work of Luque, Orozco, and co-workers, who called their version of PCM by the name MST, and who scaled the Pauling radii by 1.25 in water,[60] 1.60 in chloroform,[101] and 1.80 in carbon tetrachloride.[102] Another example of this is the UAHF model,[41] upon which the UAKS model is a variation. We

***Table 10.*** Predicted Relative Shielding Constants (ppm) using the PBE0 and B3LYP Density Functionals

| | B3LYP | | PBE0 | | |
|---|---|---|---|---|---|
| | PCM-UA0 | SM8AD | PCM-UAKS | SM8AD | experiment |
| | | | $CH_3CN$ | | |
| $CCl_4$-$C_6H_{12}$ | −0.9 | −0.7 | −0.6 | −0.7 | −1.4 |
| $CCl_4$-1,4-dioxane | −0.1 | −0.1 | NA[a] | −0.1 | 5.0 |
| $CCl_4$-$C_6H_6$ | 0.1 | 0.1 | 1.0 | 0.1 | 2.4 |
| $CCl_4$-$Et_2O$ | 4.8 | 3.5 | 5.4 | 3.6 | 2.5 |
| $CCl_4$-$CHCl_3$ | 5.4 | 3.7 | 3.9 | 3.8 | 7.3 |
| $CCl_4$-$CH_2Cl_2$ | 7.8 | 5.6 | 5.6 | 5.7 | 7.4 |
| $CCl_4$-acetone | 9.5 | 7.0 | 6.8 | 7.2 | 6.3 |
| $CCl_4$-EtOH | 9.7 | 7.2 | 13.4 | 7.3 | 11.1 |
| $CCl_4$-TFE[b] | 17.2 | 19.4 | NA | 20.2 | 21.6 |
| $CCl_4$-MeOH | 10.0 | 7.4 | 13.7 | 7.5 | 12.4 |
| $CCl_4$-$CH_3CN$ | 10.1 | 7.3 | 7.3 | 7.4 | 8.1 |
| $CCl_4$-DMSO | 10.3 | 7.6 | 7.4 | 7.7 | 6.8 |
| $CCl_4$-water[b] | 13.2 | 14.7 | 17.1 | 15.4 | 18.2 |
| MUE | 2.6 | 2.4 | NA | 2.3 | |
| | | | $CH_3NO_2$ | | |
| $CCl_4$-1,4-dioxane | 0.0 | 0.0 | NA | 0.0 | −5.3 |
| $CCl_4$-$C_6H_6$ | 0.0 | −0.1 | 0.0 | −0.1 | −2.7 |
| $CCl_4$-$Et_2O$ | −2.1 | −3.0 | 0.0 | −3.1 | −3.2 |
| $CCl_4$-$CHCl_3$ | −2.4 | −3.3 | −2.8 | −3.4 | −3.3 |
| $CCl_4$-$CH_2Cl_2$ | −3.4 | −4.8 | −7.2 | −5.0 | −3.9 |
| $CCl_4$-acetone | −4.2 | −6.1 | −2.8 | −6.3 | −6.3 |
| $CCl_4$-EtOH | −4.3 | −6.0 | −7.3 | −6.1 | −4.4 |
| $CCl_4$-MeOH | −4.4 | −6.1 | −7.0 | −6.3 | −5.1 |
| $CCl_4$-$CH_3CN$ | −4.5 | −6.7 | −3.4 | −6.8 | −6.9 |
| $CCl_4$-DMF | −4.5 | −6.2 | NA | −6.3 | −7.8 |
| $CCl_4$-DMSO | −4.6 | −6.3 | −1.6 | −6.4 | −9.1 |
| $CCl_4$-water | −4.7 | −10.3 | −3.6 | −10.5 | −9.1 |
| MUE | 2.3 | 1.5 | 2.3 | 1.5 | |
| | | | $CH_3NCS$ | | |
| $CCl_4$-$C_6H_{14}$ | 0.8 | 0.6 | NA | 0.7 | 3.2 |
| $CCl_4$-1,4-dioxane | 0.0 | 0.0 | NA | 0.0 | −2.7 |
| $CCl_4$-$C_6H_6$ | 0.0 | −0.1 | 0.0 | −0.1 | −1.1 |
| $CCl_4$-$Et_2O$ | −2.6 | −1.8 | −2.9 | −2.0 | 0.7 |
| $CCl_4$-$CHCl_3$ | −2.9 | −1.8 | −2.1 | −1.9 | −2.1 |
| $CCl_4$-acetone | −5.2 | −3.8 | −3.7 | −4.0 | −2.8 |
| $CCl_4$-$CH_2Cl_2$ | −4.2 | −2.9 | −3.0 | −3.1 | −2.0 |
| $CCl_4$-MeOH | −5.5 | −4.0 | −7.4 | −4.3 | −1.6 |
| $CCl_4$-DMSO | −5.7 | −4.2 | −4.0 | −4.4 | −6.7 |
| MUE | 2.2 | 1.8 | NA | 1.8 | |
| | | | $CH_3ONO_2$ | | |
| $CCl_4$-$C_6H_{14}$ | 0.3 | 0.4 | NA | 0.5 | 0.3 |
| $CCl_4$-1,4-dioxane | 0.0 | 0.0 | NA | 0.0 | −3.0 |
| $CCl_4$-$C_6H_6$ | 0.0 | 0.0 | 0.0 | 0.0 | −1.5 |
| $CCl_4$-$Et_2O$ | −1.0 | −1.2 | −1.2 | −1.3 | −1.5 |
| $CCl_4$-$CHCl_3$ | −1.2 | −1.6 | −0.9 | −1.6 | −1.9 |
| $CCl_4$-$CH_2Cl_2$ | −1.7 | −2.2 | −1.3 | −2.3 | −2.7 |
| $CCl_4$-acetone | −2.0 | −2.5 | −1.6 | −2.6 | −3.5 |
| $CCl_4$-TFE | −2.1 | −2.5 | NA | −2.6 | −3.9 |
| $CCl_4$-MeOH | −2.1 | −2.6 | −3.1 | −2.6 | −3.5 |
| $CCl_4$-1,2-ethanediol | −2.2 | −2.6 | NA | −2.7 | −3.9 |
| $CCl_4$-DMSO | −2.2 | −2.6 | −1.7 | −2.7 | −4.8 |
| MUE | 1.4 | 1.1 | NA | 1.1 | |
| subset MUE[c] | 2.0 | 1.5 | 1.9 | 1.5 | |
| total MUE | 2.2 | 1.7 | NA | 1.7 | |

[a] NA denotes not applicable because the method is not defined for this solvent. [b] These results were provided by cluster calculations with the solute and a single solvent molecule optimized with SM8/M06-L/6-31G(d). [c] Includes only the rows where all methods are defined.

***Table 11.*** Prediction of Relative Shielding Constants with the M06-L Functional and Continuum Solvent Models with Radii Scaled by 1.2

| | SMD | PCM-1.2B | SM8 | experiment |
|---|---|---|---|---|
| | | $CH_3CN$ | | |
| $CCl_4$-$C_6H_{12}$ | −0.6 | −0.6 | −0.5 | −1.4 |
| $CCl_4$-1,4-dioxane | 0.1 | 0.0 | 0.0 | 5.0 |
| $CCl_4$-$C_6H_6$ | 0.1 | 0.0 | 0.1 | 2.4 |
| $CCl_4$-$Et_2O$ | 3.3 | 3.0 | 2.5 | 2.5 |
| $CCl_4$-$CHCl_3$ | 3.8 | 3.4 | 2.7 | 7.3 |
| $CCl_4$-$CH_2Cl_2$ | 5.4 | 4.9 | 4.0 | 7.4 |
| $CCl_4$-acetone | 6.6 | 6.1 | 4.9 | 6.3 |
| $CCl_4$-EtOH | 6.8 | 6.2 | 4.5 | 11.1 |
| $CCl_4$-TFE[a] | 17.4 | 16.1 | 16.1 | 21.6 |
| $CCl_4$-MeOH | 7.0 | 6.4 | 4.6 | 12.4 |
| $CCl_4$-$CH_3CN$ | 7.0 | 6.4 | 5.1 | 8.1 |
| $CCl_4$-DMSO | 7.1 | 6.5 | 5.3 | 6.8 |
| $CCl_4$-water[a] | 13.8 | 12.3 | 12.0 | 18.2 |
| MUE | 2.7 | 3.0 | 3.7 | |
| | | $CH_3NO_2$ | | |
| $CCl_4$-1,4-dioxane | 0.2 | 0.0 | 0.0 | −5.3 |
| $CCl_4$-$C_6H_6$ | 0.1 | 0.0 | −0.1 | −2.7 |
| $CCl_4$-$Et_2O$ | −1.2 | −1.5 | −1.4 | −3.2 |
| $CCl_4$-$CHCl_3$ | −2.1 | −1.7 | −2.3 | −3.3 |
| $CCl_4$-$CH_2Cl_2$ | −2.6 | −2.4 | −2.9 | −3.9 |
| $CCl_4$-acetone | −2.9 | −3.0 | −3.1 | −6.3 |
| $CCl_4$-EtOH | −5.1 | −3.0 | −5.1 | −4.4 |
| $CCl_4$-MeOH | −5.8 | −3.1 | −5.7 | −5.1 |
| $CCl_4$-$CH_3CN$ | −3.3 | −3.2 | −3.4 | −6.9 |
| $CCl_4$-DMF | −2.9 | −3.2 | −3.0 | −7.8 |
| $CCl_4$-DMSO | −3.0 | −3.2 | −3.0 | −9.1 |
| $CCl_4$-$H_2O$ | −6.0 | −3.3 | −5.9 | −9.1 |
| MUE | 2.9 | 3.3 | 2.8 | |
| | | $CH_3NCS$ | | |
| $CCl_4$-$C_6H_{14}$ | 0.6 | 0.4 | 0.4 | 3.2 |
| $CCl_4$-1,4-dioxane | 0.0 | 0.0 | 0.0 | −2.7 |
| $CCl_4$-$C_6H_6$ | 0.0 | 0.0 | 0.0 | −1.1 |
| $CCl_4$-$Et_2O$ | −1.8 | −1.2 | −1.1 | 0.7 |
| $CCl_4$-$CHCl_3$ | −2.0 | −1.4 | −1.2 | −2.1 |
| $CCl_4$-$CH_2Cl_2$ | −2.9 | −2.0 | −1.7 | −2.8 |
| $CCl_4$-acetone | −3.6 | −2.5 | −2.1 | −2.0 |
| $CCl_4$-MeOH | −3.8 | −2.7 | −2.1 | −1.6 |
| $CCl_4$-DMSO | −3.9 | −2.7 | −2.3 | −6.7 |
| MUE | 1.7 | 1.6 | 1.7 | |
| | | $CH_3ONO_2$ | | |
| $CCl_4$-$C_6H_{14}$ | 0.3 | 0.2 | 0.2 | 0.3 |
| $CCl_4$-1,4-dioxane | 0.1 | 0.0 | 0.0 | −3.0 |
| $CCl_4$-$C_6H_6$ | 0.0 | 0.0 | −0.0 | −1.5 |
| $CCl_4$-$Et_2O$ | −0.6 | −0.7 | −0.6 | −1.5 |
| $CCl_4$-$CHCl_3$ | −1.0 | −0.8 | −0.9 | −1.9 |
| $CCl_4$-$CH_2Cl_2$ | −1.3 | −1.2 | −1.1 | −2.7 |
| $CCl_4$-acetone | −1.4 | −1.4 | −1.5 | −3.5 |
| $CCl_4$-TFE | −2.6 | −1.5 | −1.0 | −3.9 |
| $CCl_4$-MeOH | −2.6 | −1.5 | −1.0 | −3.5 |
| $CCl_4$-1,2-ethanediol | −2.7 | −1.6 | −1.1 | −3.9 |
| $CCl_4$-DMSO | −1.5 | −1.6 | −1.2 | −4.8 |
| MUE | 1.5 | 1.8 | 2.0 | |
| total MUE | 2.3 | 2.5 | 2.6 | |

[a] These results were provided by cluster calculations with the solute and a single solvent molecule optimized with SM8/M06-L/6-31G(d).

test the PCM-MST method in Table 12, which—unlike other tables—shows *errors* in shielding constants, not shielding constants. This approach does much better than other models (except clustered SMD) for the $CCl_4$-$H_2O$ shift of $CH_3CN$. Overall, PCM-MST is better than PCM-1.2B for $CC1_4$-$H_2O$ shifts, but it is consistently worse for $CCl_4$-$CHCl_3$ shifts. Comparing PCM-MST and the SM*x* models on a case by case basis, for the cases in Table 12, excluding the bare solute row, SMD performs the best, and SM8, SM8AD, and PCM-MST perform about equally well. In view of the limited number of solvents for which this test is possible, we will draw our final conclusions based on the mean unsigned errors for the larger and more diverse sets of solvents.

***Table 12.*** Magnitudes of the Errors in Calculated $^{14}N$ Shielding Constants, Relative to Their Values in $CCl_4$

| | PCM-MST | SM8 | SMD | SM8AD | PCM-UA0 | PCM-UAKS | PCM-1.2B |
|---|---|---|---|---|---|---|---|
| | | | $CH_3CN$ | | | | |
| $CCl_4$-$CHCl_3$ | 3.1 | 2.9 | 1.3 | 4.0 | 2.3 | 3.8 | 1.9 |
| $CCl_4$-$H_2O$ (bare solute) | 2.6 | 10.2 | 6.4 | 12.4 | 8.6 | 5.4 | 7.6 |
| $CCl_4$-$H_2O$ (cluster) | 1.4 | 4.2 | 1.1 | 5.0 | 5.9 | 3.1 | 4.2 |
| | | | $CH_3NO_2$ | | | | |
| $CCl_4$-$CHCl_3$ | 1.0 | 0.5 | 0.0 | 0.2 | 1.1 | 1.6 | 0.7 |
| $CCl_4$-$H_2O$ | 0.2 | 0.3 | 0.0 | 0.4 | 4.8 | 2.3 | 3.9 |
| | | | $CH_3NCS$ | | | | |
| $CCl_4$-$CHCl_3$ | 0.5 | 0.5 | 1.1 | 0.3 | 0.6 | 0.2 | 0.2 |
| | | | $CH_3ONO_2$ | | | | |
| $CCl_4$-$CHCl_3$ | 0.9 | 0.7 | 0.4 | 0.6 | 0.9 | 1.2 | 0.7 |

*6.D.3. Solvent Shifts Relative to $CCl_4$ - Extended Basis Set Results.* In order to test if an increase in the basis set size would give more accurate results for NPE-solvers, we undertook additional calculations for the entire test set at the SMD/M06-L/6-311++G(2df,2p) and SMD/M06-L/111111−31G(d) levels, where the latter is a decontracted version of the 6-31G(d) basis set. Results are presented in Table 13.

Table 13 shows that increasing the basis set size by decontracting core functions does not increase the accuracy of the model tested here. Almost no difference in the mean errors is seen for the methods that used the contracted and decontracted versions of the 6-31G(d) basis set, which illustrates the small effect of core functions in isotropic shielding constants. Indeed, the average change in absolute nuclear shielding upon this decontraction is only 0.3 ppm.

SMD/M06-L/6-311++G(2df,2p) show slight improvements for methyl nitrate and nitromethane, but the opposite is observed for acetonitrile and methyl isothiocyanate, and the total mean unsigned error for this method is 20% larger than when 6-31G(d) is used as the basis set in either its decontracted or standard version. As noted above in section 6.A, we ascribe this decrease in accuracy to the greater charge penetration outside of the solute cavity with the larger basis set. Table 14 lists the errors on total polarization charges (i.e., the amount by which the $q_m$ failed to satisfy eq 7) for each solute in each solvent for the SMD model with the 6-31G(d) and 6-311++G(2df,2p) basis sets; these provide some measure of the amount of outlying charge, and larger errors—up to 50% larger—are found for 6-311++G(2df,2p) in every case. We conclude that the smaller basis set results are likely to be more physical.

## 7. Additional Discussion

It has been emphasized in previous work[35,103,104] that there is no fundamental way to separate electrostatic and nonelectrostatic contributions to solvation. The long-range effects of bulk solvent can be estimated quite reasonably from the bulk dielectric constant, so the questionable contributions are all localized to the nearby solvent and are dominated by the first solvation shell.[28] Provided, though, that nonelectrostatic terms dependent on the nature and extent of first-solvation-shell effects are optimized to be consistent with a systematic and well-defined scheme for bulk-electrostatic effects, one can obtain good across-the-board accuracy for free energies of solvation in both aqueous and diverse nonaqueous media.[28−34,104] However in SCRF models, only the terms treated self-consistently have an effect on the electronic properties of the solute (for a given solute geometry), and all widely used methods for calculating solvation energies treat only the bulk-electrostatic terms self-consistently.[36,37] Since one can obtain reasonable solvation free energies without carrying out self-consistent calculations even when one underestimates or neglects the electrostatic contributions,[105,106] obtaining accurate solvation free energies does not guarantee accurate response of solute properties to the density,[103,104] and separate tests are necessary. However it is not clear what properties of the solute can provide definitive tests. For example, the partial atomic charges of the solute provide a clear physical picture of solute polarization,[107] but they are not physically observable. The dipole moment of a solute molecule is a physical observable in the gas phase, and it is sensitive to solute response,[103] but it is not precisely defined in solution because there is no unique way to divide electron density between the solute and the solvent. Zhan and Chipman[16] have suggested that the solvent dependence of NMR chemical shielding at nitrogen can be used to evaluate the treatment of solute electron-density response, and we have adopted their suggestion in the present work.

In practical work the extent of predicted solute polarization is primarily controlled by the choice of cavity size and shape, where the solute cavity is defined as the region in which the dielectric constant is unity; the dielectric constant is set equal to the bulk value outside the cavity. In the SM*x* models we have optimized the parameters that control the cavity size and shape primarily to free energies of solvation of ions,[108] both clustered with explicit solvent molecules[109,110] and unclustered; since these quantities are dominated by bulk electrostatics, this provides a realistic way to pin down the partition into bulk electrostatic effects and other effects. The PCM solvation models have used other criteria for cavity parameters.[37,41,44,60−64,101,102] In fact, the multitude of cavity definition protocols in modern continuum solvation models, including some which adjust atomic radii as a function of partial atomic charge (a choice not adopted in the SMx models), attests to the lack of consensus on what is the most realistic way to define the cavities. The present study to confirm the usefulness of the approach adopted in the SMx models is therefore useful.

***Table 13.*** Prediction of Relative Shielding Constants with SMD/M06-L/6-311++G(2df,2p) and SMD/M06-L/111111-31G(d)

| | SMD/ 111111−31G(d) | SMD/ 6-311++G(2df,2p) | experiment |
|---|---|---|---|
| | $CH_3CN$ | | |
| $CCl_4$-$C_6H_{12}$ | −1.0 | −2.2 | −1.4 |
| $CCl_4$-1,4-dioxane | −0.1 | −0.1 | 5.0 |
| $CCl_4$-$C_6H_6$ | 0.1 | 0.1 | 2.4 |
| $CCl_4$-$Et_2O$ | 5.3 | 6.6 | 2.5 |
| $CCl_4$-$CHCl_3$ | 6.0 | 7.5 | 7.3 |
| $CCl_4$-$CH_2Cl_2$ | 8.6 | 10.9 | 7.4 |
| $CCl_4$-acetone | 10.6 | 13.4 | 6.3 |
| $CCl_4$-EtOH | 10.9 | 13.7 | 11.1 |
| $CCl_4$-TFE[a] | 18.3 | 19.0 | 21.6 |
| $CCl_4$-MeOH | 11.2 | 14.1 | 12.4 |
| $CCl_4$-$CH_3CN$ | 11.3 | 14.3 | 8.1 |
| $CCl_4$-DMSO | 11.5 | 14.5 | 6.8 |
| $CCl_4$-water[a] | 15.7 | 16.7 | 18.2 |
| MUE | 2.5 | 3.5 | |
| MUE (6-31G(d)) | 2.4 | | |
| | $CH_3NO_2$ | | |
| $CCl_4$-1,4-dioxane | 0.3 | 0.3 | −5.3 |
| $CCl_4$-$C_6H_6$ | 0.2 | 0.3 | −2.7 |
| $CCl_4$-$Et_2O$ | −2.0 | −2.4 | −3.2 |
| $CCl_4$-$CHCl_3$ | −3.3 | −3.8 | −3.3 |
| $CCl_4$-$CH_2Cl_2$ | −4.3 | −5.0 | −3.9 |
| $CCl_4$-acetone | −4.8 | −5.6 | −6.3 |
| $CCl_4$-EtOH | −7.9 | −8.8 | −4.4 |
| $CCl_4$-MeOH | −8.7 | −9.5 | −5.1 |
| $CCl_4$-$CH_3CN$ | −5.3 | −6.2 | −6.9 |
| $CCl_4$-DMF | −4.8 | −5.7 | −7.8 |
| $CCl_4$-DMSO | −4.9 | −5.8 | −9.1 |
| $CCl_4$-$H_2O$ | −9.0 | −9.9 | −9.1 |
| MUE | 2.3 | 2.3 | |
| MUE(6-31G(d)) | 2.3 | | |
| | $CH_3NCS$ | | |
| $CCl_4$-$C_6H_{14}$ | 0.9 | 1.0 | 3.2 |
| $CCl_4$-1,4-dioxane | 0.0 | 0.0 | −2.7 |
| $CCl_4$-$C_6H_6$ | 0.0 | 0.0 | −1.1 |
| $CCl_4$-$Et_2O$ | −2.8 | −3.3 | 0.7 |
| $CCl_4$-$CHCl_3$ | −3.2 | −3.7 | −2.1 |
| $CCl_4$-$CH_2Cl_2$ | −4.7 | −5.4 | −2.8 |
| $CCl_4$-acetone | −5.8 | −6.7 | −2.0 |
| $CCl_4$-MeOH | −6.1 | −7.0 | −1.6 |
| $CCl_4$-DMSO | −6.2 | −7.2 | −6.7 |
| MUE | 2.4 | 2.8 | |
| MUE(6-31G(d)) | 2.4 | | |
| | $CH_3ONO_2$ | | |
| $CCl_4$-$C_6H_{14}$ | 0.4 | 0.5 | 0.3 |
| $CCl_4$-1,4-dioxane | 0.1 | 0.1 | −3.0 |
| $CCl_4$-$C_6H_6$ | 0.1 | 0.1 | −1.5 |
| $CCl_4$-$Et_2O$ | −1.0 | −1.2 | −1.5 |
| $CCl_4$-$CHCl_3$ | −1.6 | −1.8 | −1.9 |
| $CCl_4$-$CH_2Cl_2$ | −2.0 | −2.4 | −2.7 |
| $CCl_4$-acetone | −2.2 | −2.7 | −3.5 |
| $CCl_4$-TFE | −3.8 | −4.2 | −3.9 |
| $CCl_4$-MeOH | −3.8 | −4.3 | −3.5 |
| $CCl_4$-1,2-ethanediol | −3.9 | −4.3 | −3.9 |
| $CCl_4$-DMSO | −2.3 | −2.7 | −4.8 |
| MUE | 1.0 | 0.8 | |
| MUE (6-31G(d)) | 1.0 | | |
| total MUE | 2.0 | 2.4 | |
| total MUE(6-31G(d)) | 2.0 | | |

[a] These results were provided by cluster calculations with the solute and a single solvent molecule optimized with SM8/M06-L/6-31G(d).

***Table 14.*** Error on Total Polarization Charges (in au) Given by the Methods SMD/M06-L/6-31G(d) and SMD/M06-L/6-311++G(2df,2p)

| | SMD/6-31G(d) | SMD/6-311++G(2df,2p) |
|---|---|---|
| | $CH_3CN$ | |
| $C_6H_{12}$ | 0.008 | 0.010 |
| 1,4-dioxane | 0.009 | 0.011 |
| $C_6H_6$ | 0.009 | 0.011 |
| $CCl_4$ | 0.009 | 0.011 |
| $Et_2O$ | 0.012 | 0.015 |
| $CHCl_3$ | 0.012 | 0.016 |
| $CH_2Cl_2$ | 0.014 | 0.018 |
| acetone | 0.014 | 0.019 |
| EtOH | 0.015 | 0.019 |
| TFE | 0.015 | 0.019 |
| MeOH | 0.015 | 0.019 |
| $CH_3CN$ | 0.015 | 0.019 |
| DMSO | 0.015 | 0.019 |
| $H_2O$ | 0.015 | 0.020 |
| average | 0.012 | 0.016 |
| | $CH_3NO_2$ | |
| 1,4-dioxane | 0.004 | 0.005 |
| $C_6H_6$ | 0.004 | 0.005 |
| $CCl_4$ | 0.004 | 0.005 |
| $Et_2O$ | 0.006 | 0.007 |
| $CHCl_3$ | 0.007 | 0.009 |
| $CH_2Cl_2$ | 0.007 | 0.009 |
| acetone | 0.007 | 0.009 |
| EtOH | 0.015 | 0.022 |
| MeOH | 0.020 | 0.028 |
| $CH_3CN$ | 0.007 | 0.009 |
| DMF | 0.007 | 0.008 |
| DMSO | 0.007 | 0.008 |
| $H_2O$ | 0.020 | 0.029 |
| average | 0.009 | 0.012 |
| | $CH_3NCS$ | |
| $C_6H_{14}$ | 0.008 | 0.009 |
| 1,4-dioxane | 0.007 | 0.008 |
| $C_6H_6$ | 0.008 | 0.009 |
| $CCl_4$ | 0.008 | 0.009 |
| $Et_2O$ | 0.011 | 0.013 |
| $CHCl_3$ | 0.011 | 0.013 |
| $CH_2Cl_2$ | 0.013 | 0.015 |
| acetone | 0.014 | 0.016 |
| MeOH | 0.014 | 0.016 |
| DMSO | 0.014 | 0.014 |
| average | 0.011 | 0.012 |
| | $CH_3ONO_2$ | |
| $CCl_4$ | 0.004 | 0.005 |
| $C_6H_{14}$ | 0.003 | 0.004 |
| 1,4-dioxane | 0.004 | 0.005 |
| $C_6H_6$ | 0.004 | 0.005 |
| $Et_2O$ | 0.005 | 0.006 |
| $CHCl_3$ | 0.007 | 0.009 |
| $CH_2Cl_2$ | 0.007 | 0.009 |
| acetone | 0.007 | 0.008 |
| TFE | 0.021 | 0.029 |
| MeOH | 0.021 | 0.029 |
| 1,2-ethanediol | 0.022 | 0.029 |
| DMSO | 0.007 | 0.008 |
| average | 0.009 | 0.012 |
| total average | 0.010 | 0.013 |

Hydrogen bonding between the solute and solvent is the classic example of a solute−solvent interaction with atomic-scale character that cannot be understood entirely in terms of bulk solvent properties. And yet even hydrogen bonding is often dominated by electrostatics.[111] One particularly informative study of the solvent effect on an NMR nuclear shielding of a hydrogen-bonded system is the study of the $^{17}O$ chemical shielding in acetone by Aidas et al.[112] They found that the gas-to-water solvent shift is underestimated by 22 pm (30%) by the PCM-UA0 model. They pointed out that it had been suggested[17,21,113] that larger cavities might be employed in the PCM model to improve the calculated shieldings but that larger cavities would make the agreement

worse. To obtain a more accurate value, they instead employed a procedure combining several elements. First they sampled 700 configurations of acetone in water in a molecular dynamics simulation with explicit water molecules. For each configuration they then carried out an SCRF calculation on a supersolute consisting of acetone and the two closest water molecules, which yielded widely distributed values with a standard deviation from the mean of 13 ppm. Averaging over these values yields a shift of 76.5 ppm, which happens to be within 1.1 ppm of experiment. In the standard approach one attempts to find a cavity definition where a calculation at a single representative solute geometry (and often with only implicit water) yields the average result directly. Here we use one explicit water when there is hydrogen bonding of the solvent to the atom at which the chemical shift is measured, but nevertheless the large spread of values found for instantaneous solvent configurations in the work of Aidas et al. shows why it is hard to capture the effect of a specific hydrogen bonding interaction with a calculation for a single solute−solvent configuration.

## 8. Conclusions

Several combinations of continuum solvation models and density functionals were assessed for their ability to predict the solvent dependence of 49 $^{14}$N chemical shifts in four different solutes and seventeen different solvents. We conclude the following from our results:

(1) The continuum solvent models do not give particularly reliable predictions of the solvent shifts; errors range from about 1.7 to 3.0 ppm depending on the model. In part this reflects the importance of specific solute−solvent interactions, but if we nevertheless ask which existing continuum solvation model is best (smallest mean unsigned errors) for computing the solvent dependence of $^{14}$N chemical shifts, we find that the generalized Born models SM8 and SM8AD, used with their standard values for the intrinsic Coulomb radii, perform the best-despite the fact that these models were optimized for the computation of molecular free energies of solvation. SMD and PCM-1.2B, which determine the reaction field from approximate solution of the nonhomogeneous Poisson equation, also give better results when their standard radii are used. Although earlier studies[21,22] scaled standard radii by factors greater than one, and the fitting approach presented in section 6.C suggested that this could be a useful way of improving the solvent shifts predicted by NPE-based models, this approach did not improve the accuracy of solvent shifts computed relative to carbon tetrachloride.

(2) Including a specific solvent molecule in a solute−solvent cluster improves predicted $^{14}$N chemical shifts when a strong hydrogen bond is made from the solvent molecule to the nitrogen atom of the solute.

(3) All SM*x* models correctly predict the positive or negative dielectric dependence of the solvent shifts in all four solutes studied here, $CH_3CN$, $CH_3NO_2$, $CH_3NCS$, and $CH_3ONO_2$, in contrast to previous findings with the SVPE and SPE methods.

(4) Increasing the basis set size for PCM-based models does not improve the calculation of NMR chemical shifts in solution, as larger basis sets including diffuse functions lead to larger quantities of outlying charge. In PCM-based models, such outlying charge contributes to unphysical effects on computed nuclear shieldings.

(5) The SM8 and SM8AD solvation models offered the most quantitatively accurate results compared to experiment when solvent-to-solvent shifts were examined. Most calculations were carried out with the M06-L density functional, but substitution of B3LYP or PBE0 for M06-L gave slightly improved accuracy in the case of SM8AD. Solvation models such as PCM that are based on a reaction field determined from an approximate solution of the nonhomogeneous Poisson equation showed somewhat reduced accuracy. The success of the SM*x* models is encouraging because the SM*x* models also provide excellent accuracy for free energies of solvation,[31−34] much better for example than does the default version of PCM in *Gaussian03*.

It thus appears that the Coulomb radii normally used to predict free energies of solvation in the SM*x* models are also the most appropriate ones for predicting NMR shielding constants in solution and that those solvation models that do best for free energies of solvation are also reasonable choices for property calculations. It will be interesting in the future to identify other well-defined solvent response properties that will permit this question to be assessed in more detail.

**Acknowledgment.** The authors are grateful to Roberto Cammi and Daniel Chipman for many stimulating discussions. This work was supported in part by the National Science Foundation under grant nos. CHE06-10183 and CHE07-04974.

**Supporting Information Available:** Plots of the dependence on dielectric constant of the relative nitrogen shielding calculated by the scaled radii SMx models. This material is available free of charge via the Internet at http://pubs.acs.org.

### References

(1) Pople, J. A.; Schneider, W. G.; Bernstein, H. J. *High Resolution Nuclear Magnetic Resonance*. McGraw-Hill: New York, 1959.

(2) Emsley, J. W.; Feeney, J.; Sutcliffe, L. H. *High Resolution Nuclear Magnetic Resonance Spectroscopy*; Pergamon Press: 1965; Vol. 1.

(3) Ando, I.; Webb, G. A. *Theory of NMR Parameters*; Academic Press: New York, 1983.

(4) Buckingham, A. D.; Schaefer, T.; Schneider, W. G. *J. Chem. Phys.* **1960**, *32*, 1227.

(5) Kamlet, M. J.; Abboud, J. L. M.; Abraham, M. H.; Taft, R. W. *J. Org. Chem.* **1983**, *48*, 2877.

(6) Begtrup, M.; Taft, R. W.; Kamlet, M. J. *J. Org. Chem.* **1986**, *51*, 2130.

(7) Witanowski, M.; Sitkowski, J.; Biernat, S.; Kamienski, B.; Hamdi, B. T.; Webb, G. A. *Magn. Reson. Chem.* **1985**, *23*, 748.

(8) Witanowski, M.; Sitkowski, J.; Biernat, S.; Sudha, L. V.; Webb, G. A. *Magn. Reson. Chem.* **1987**, *25*, 725.

(9) Witanowski, M.; Sicinska, W.; Webb, G. A. *Magn. Reson. Chem.* **1989**, *27*, 380.

(10) Witanowski, M.; Stefaniak, L.; Webb, G. A. In *Annual Reports on NMR spectroscopy*; Webb, G. A., Ed.; Academic Press: London, 1993, Vol. 25, p. 86.

(11) Witanowski, M.; Sicinska, W.; Biedrzycka, Z.; Grabowski, Z.; Webb, G. A. *J. Magn. Reson. A* **1995**, *112*, 66.

(12) Witanowski, M.; Biedrzycka, Z.; Sicinska, W.; Grabowski, Z. *J. Magn. Reson.* **2003**, *164*, 212.

(13) Alkorta, I.; Elguero, J. *Struct. Chem.* **2003**, *14*, 377.

(14) Bagno, A.; Rastrelli, F.; Saielli, G. *Prog. Nucl. Magn. Reson. Spectrosc.* **2005**, *47*, 41.

(15) Cammi, R. *J. Chem. Phys.* **1998**, *109*, 3185.

(16) Zhan, C.-G.; Chipman, D. M. *J. Chem. Phys.* **1999**, *110*, 1611.

(17) Cammi, R.; Mennucci, B.; Tomasi, J. *J. Chem. Phys.* **1999**, *110*, 7627.

(18) Jaszuński, M.; Mikkelsen, K. V.; Rizzo, A.; Witanowski, M. *J. Phys Chem. A* **2000**, *104*, 1466.

(19) Manalo, M. N.; de Dios, A. C.; Cammi, R. *J. Phys. Chem. A* **2000**, *104*, 9600.

(20) Ksiazek, A.; Borowski, P.; Wolinski, K. *J. Magn. Reson.* **2009**, *197*, 153.

(21) Mennucci, B.; Martinez, J. M.; Tomasi, J. *J. Phys. Chem. A* **2001**, *105*, 7287.

(22) Mennucci, B. *J. Am. Chem. Soc.* **2002**, *124*, 1506.

(23) Fazaeli, R.; Monajjemi, M.; Ataherian, F.; Zare, K. *THEOCHEM* **2002**, *581*, 51.

(24) Manalo, M. N.; de Dios, A. C. *Magn. Reson. Chem.* **2002**, *40*, 781.

(25) Chipman, D. M. *Theor. Chem. Acc.* **2004**, *111*, 61.

(26) Bulo, R. E.; Jacob, C. R.; Visscher, L. *J. Phys. Chem. A* **2008**, *112*, 2640.

(27) Cramer, C. J.; Truhlar, D. G. *J. Am. Chem. Soc.* **1991**, *113*, 8305.

(28) Cramer, C. J.; Truhlar, D. G. *Science* **1992**, *256*, 213.

(29) Giesen, D. J.; Gu, M. Z.; Cramer, C. J.; Truhlar, D. G. *J. Org. Chem.* **1996**, *61*, 8720.

(30) Kelly, C. P.; Cramer, C. J.; Truhlar, D. G. *J. Chem. Theory Comput.* **2005**, *1*, 1133.

(31) Marenich, A. V.; Olson, R. M.; Kelly, C. P.; Cramer, C. J.; Truhlar, D. G. *J. Chem. Theory Comput.* **2007**, *3*, 2011.

(32) Cramer, C. J.; Truhlar, D. G. In *Trends and Perspectives in Modern Computational Science, Lecture Series on Computer and Computational Sciences Volume 6*; edited by Maroulis, G., Simos,T. E., Ed.; Brill/VSP: Leiden, 2006; pp 112−139. Cramer, C. J.; Truhlar, D. G. *Acc. Chem. Res.* **2008**, *41*, 760.

(33) Marenich, A. V.; Cramer, C. J.; Truhlar, D. G. *J. Phys. Chem. B* **2009**, *113*, 6378.

(34) Marenich, A. V.; Cramer, C. J.; Truhlar, D. G. *J. Chem. Theory Comput.,* in press.

(35) Marenich, A. V.; Cramer, C. J.; Truhlar, D. G. *J. Chem. Theory Comput.* **2008**, *4*, 877.

(36) Cramer, C. J.; Truhlar, D. G. *Chem. Rev.* **1999**, *99*, 2161.

(37) Tomasi, J.; Mennucci, B.; Cammi, R. *Chem. Rev.* **2005**, *105*, 2999.

(38) Miertuŝ, S.; Scrocco, E.; Tomasi, J. *Chem. Phys.* **1981**, *55*, 117.

(39) Cancés, E.; Mennucci, B.; Tomasi, J. *J. Chem. Phys.* **1997**, *107*, 3032.

(40) Tomasi, J.; Mennucci, B.; Cancès, E. *J. Mol. Struct. THEOCHEM* **1999**, *464*, 211.

(41) Barone, V.; Cossi, M.; Tomasi, J. *J. Chem. Phys.* **1997**, *107*, 3210.

(42) Cossi, M.; Scalmani, G.; Rega, N.; Barone, V. *J. Chem. Phys.* **2002**, *117*, 43.

(43) Cossi, M.; Rega, N.; Scalmani, G.; Barone, V. *J. Comput. Chem.* **2003**, *24*, 669.

(44) Barone, V.; Improta, R.; Rega, N. *Theor. Chem. Acc.* **2004**, *111*, 237.

(45) Frisch, M. J.; Trucks, G. W.; Schlegel, H. B.; Scuseria, G. E.; Robb, M. A.; Cheeseman, J. R.; Montgomery, J. A., Jr.; Vreven, T.; Kudin, K. N.; Burant, J. C.; Millam, J. M.; Iyengar, S. S.; Tomasi, J.; Barone, V.; Mennucci, B.; Cossi, M.; Scalmani, G.; Rega, N.; Petersson, G. A.; Nakatsuji, H.; Hada, M.; Ehara, M.; Toyota, K.; Fukuda, R.; Hasegawa, J.; Ishida, M.; Nakajima, T.; Honda, Y.; Kitao, O.; Nakai, H.; Klene, M.; Li, X.; Knox, J. E.; Hratchian, H. P.; Cross, J. B.; Bakken, V.; Adamo, C.; Jaramillo, J.; Gomperts, R.; Stratmann, R. E.; Yazyev, O.; Austin, A. J.; Cammi, R.; Pomelli, C.; Ochterski, J. W.; Ayala, P. Y.; Morokuma, K.; Voth, G. A.; Salvador, P.; Dannenberg, J. J.; Zakrzewski, V. G.; Dapprich, S.; Daniels, A. D.; Strain, M. C.; Farkas, O.; Malick, D. K.; Rabuck, A. D.; Raghavachari, K.; Foresman, J. B.; Ortiz, J. V.; Cui, Q.; Baboul, A. G.; Clifford, S.; Cioslowski, J.; Stefanov, B. B.; Liu, G.; Liashenko, A.; Piskorz, P.; Komaromi, I.; Martin, R. L.; Fox, D. J.; Keith, T.; Al-Laham, M. A.; Peng, C. Y.; Nanayakkara, A.; Challacombe, M.; Gill, P. M. W.; Johnson, B.; Chen, W.; Wong, M. W.; Gonzalez, C.; and Pople, J. A. *Gaussian03, revision E.01*; Gaussian, Inc.: Pittsburgh, PA, 2003.

(46) Schmidt, M. W.; Baldridge, K. K.; Boatz, J. M.; Elbert, S. T.; Gordon, M. S.; Jensen, J. H.; Koseki, S.; Matsunaga, N.; Nguyen, K. A.; Su, S.; Windus, T. L.; Dupuis, M.; Montgomery, J. A. *J. Comput. Chem.* **1993**, *14*, 1347.

(47) *Chemical Applications of Atomic and Molecular Electrostatic Potentials*; Politzer, P., Truhlar, D. G., Eds.; Plenum: New York, 1981.

(48) Cramer, C. J.; Truhlar, D. G. In *Free Energy Calculations in Rational Drug Design*; Reddy, M. R., Erion, M. D., Eds.; Kluwer/Plenum: New York, 2001; p 63.

(49) Hoijtink, G. J.; de Boer, E.; van der Meij, P. H.; Weijland, W. P. *Recl. Trav. Chim. Pays-Bas Belg.* **1956**, *75*, 487.

(50) Peradejordi, F. *Cah. Phys.* **1963**, *17*, 393.

(51) Jano, I. *C. R. Acad. Sci.(Paris)* **1965**, *261*, 103.

(52) Tucker, S. C.; Truhlar, D. G. *Chem. Phys. Lett.* **1989**, *157*, 164.

(53) Still, W. C.; Tempczyk, A.; Hawley, R. C.; Hendrickson, T. *J. Am. Chem. Soc.* **1990**, *112*, 6127.

(54) Cramer, C. J.; Truhlar, D. G. *Rev. Comp. Chem.* **1995**, *6*, 1.

(55) Liotard, D. A.; Hawkins, G. D.; Lynch, G. C.; Cramer, C. J.; Truhlar, D. G. *J. Comput. Chem.* **1995**, *16*, 422.

(56) Grycuk, T. *J. Chem. Phys.* **2003**, *119*, 4817.

(57) Storer, J. W.; Giesen, D. J.; Cramer, C. J.; Truhlar, D. G. *J. Comput.-Aided Mol. Des.* **1995**, *9*, 87.

(58) Olson, R. M.; Marenich, A. V.; Cramer, C. J.; Truhlar, D. G. *J. Chem. Theory Comput.* **2007**, *3*, 2046.

(59) Bondi, A. *J. Phys. Chem.* **1964**, *68*, 441.

(60) Bachs, M.; Luque, F. J.; Orozco, M. *J. Comput. Chem.* **1994**, *15*, 446.

(61) Tomasi, J.; Persico, M. *Chem. Rev.* **1994**, *94*, 2027.

(62) Mennucci, B.; Cossi, M.; Tomasi, J. *J. Chem. Phys.* **1995**, *102*, 6837.

(63) Klamt, A.; Jonas, V.; Bürger, T.; Lohrenz, J. C. W. *J. Phys. Chem. A* **1998**, *102*, 5074.

(64) Klamt, A.; Eckert, F. *Fluid Phase Equilib.* **2000**, *172*, 43.

(65) Chipman, D. M. *J. Chem. Phys.* **1997**, *106*, 10194.

(66) Zhan, C.-G.; Bentley, J.; Chipman, D. M. *J. Chem. Phys.* **1998**, *108*, 177.

(67) Helgaker, T.; Jaszunski, M.; Ruud, K. *Chem. Rev.* **1999**, *99*, 293.

(68) Jameson, C. J.; de Dios, A. C. *Nucl. Magn. Reson.* **2003**, *32*, 43.

(69) Facelli, J. C. *Concepts Magn. Reson.* **2004**, *20A*, 42.

(70) Izgorodina, E. I.; Brittain, D. R. B.; Hodgson, J. L.; Krenske, E. H.; Lin, C. Y.; Namazian, M.; Coote, M. L. *J. Phys. Chem. A* **2007**, *111*, 10754.

(71) Ditchfield, R. *Mol. Phys.* **1974**, *27*, 789.

(72) Wolinski, K.; Hinton, J. F.; Pulay, P. *J. Am. Chem. Soc.* **1990**, *112*, 8251.

(73) Kutzelnigg, W. *Isr. J. Chem.* **1980**, *19*, 193.

(74) Keith, T. A.; Bader, R. F. W. *Chem. Phys. Lett.* **1993**, *210*, 223.

(75) Lazzeretti, P.; Malagoli, M.; Zanasi, R. *Chem. Phys. Lett.* **1994**, *220*, 299.

(76) Ligabue, A.; Sauer, S. P. A.; Lazzeretti, P. *J. Chem. Phys.* **2007**, *126*, 154111.

(77) Zhao, Y.; Truhlar, D. G. *MN-GFM: Minnesota Gaussian Functional Module, version 4.1*; University of Minnesota: Minneapolis, MN, 2008.

(78) *MN-GSM-v2009: Minnesota Gaussian Solvation Module, version 2009*; University of Minnesota: Minneapolis, MN, 2009.

(79) Zhao, Y.; Truhlar, D. G. *Theor. Chem. Acc.* **2008**, *120*, 215.

(80) Zhao, Y.; Truhlar, D. G. *J. Phys. Chem. A* **2008**, *112*, 6794.

(81) Cheeseman, J. R.; Trucks, G. W.; Keith, T. A.; Frisch, M. J. *J. Chem. Phys.* **1996**, *104*, 5497.

(82) Bachrach, S. M. In *Reviews in Computational Chemistry*; Lipkowitz, K. B., Boyd, D. B., Eds.; VCH: 1994; Vol. 5. pp 171−228.

(83) Chesnut, D. B.; Rusiloski, B. E. *J. Mol. Struct. THEOCHEM* **1994**, *314*, 19. Schreckenbach, G.; Ziegler, T. *J. Phys. Chem.* **1995**, *99*, 606.

(84) Astrand, P.-O.; Mikkelsen, K. V.; Jorgensen, P.; Ruud, K.; Helgaker, T. *J. Chem. Phys.* **1998**, *108*, 2528.

(85) Abraham, M. H. *Chem. Soc. Rev.* **1993**, *22*, 73.

(86) Binkley, J. S.; Pople, J. A.; Hehre, W. J. *J. Am. Chem. Soc.* **1980**, *102*, 939.

(87) Gordon, M. S.; Binkley, J. S.; Pople, J. A.; Pietro, W. J.; Hehre, W. J. *J. Am. Chem. Soc.* **1982**, *104*, 2797.

(88) Krishnan, R.; Binkley, J. S.; Seeger, R.; Pople, J. A. *J. Chem. Phys.* **1980**, *72*, 650.

(89) Frisch, M. J.; Pople, J. A.; Binkley, J. S. *J. Chem. Phys.* **1984**, *80*, 3265.

(90) Davidson, E. R.; Feller, D. *Chem. Rev.* **1986**, *86*, 681.

(91) Jensen, F. *J. Chem. Theory Comput.* **2008**, *4*, 719.

(92) Feller, D. *J. Comput. Chem.* **1996**, *17*, 1571.

(93) Schuchardt, K. L.; Didier, B. T.; Elsethagen, T.; Sun, L.; Gurumoorthi, V.; Chase, J.; Li, J.; Windus, T. L. *J. Chem. Inf. Model.* **2007**, *47*, 1045.

(94) Winget, P.; Dolney, D. M.; Giesen, D. J.; Cramer, C. J.; Truhlar, D. G. Minnesota Solvent Descriptor Database. http://comp.chem.umn.edu/solvation/mnsddb.pdf (accessed May 1, 2009).

(95) Becke, A. D. *J. Chem. Phys.* **1993**, *98*, 5648.

(96) Lee, C.; Yang, W.; Parr, R. G. *Phys. Rev. B* **1988**, *37*, 785.

(97) Vosko, S. H.; Wilk, L.; Nusair, M. *Can. J. Phys.* **1980**, *58*, 1200.

(98) Stephens, P. J.; Devlin, F. J.; Chabalowski, C. F.; Frisch, M. J. *J. Phys. Chem.* **1994**, *98*, 11623.

(99) Adamo, C.; Barone, V. *Chem. Phys. Lett.* **1998**, *298*, 113.

(100) Klamt, A.; Mennucci, B.; Tomasi, J.; Barone, V.; Curutchet, C.; Orozco, M.; Luque, F. J. *Acc. Chem. Res.* **2009**, *42*, 489.

(101) Luque, F. J.; Zhang, Y.; Aleman, C.; Bachs, M.; Gao, J.; Orozco, M. *J. Phys. Chem.* **1996**, *100*, 4269.

(102) Luque, F. J.; Bachs, M.; Aleman, C.; Orozco, M. *J. Comput. Chem.* **1996**, *17*, 806.

(103) Curutchet, C.; Cramer, C. J.; Truhlar, D. G.; Ruiz-Lopez, M. F.; Rinaldi, D.; Orozco, M.; Luque, F. J. *J. Comput. Chem.* **2003**, *24*, 284.

(104) Cramer, C. J.; Truhlar, D. G. *Acc. Chem. Res.* **2009**, *42*, 493.

(105) Hawkins, G. D.; Cramer, C. J.; Truhlar, D. G. *J. Phys. Chem. B* **1997**, *101*, 7147.

(106) Hawkins, G. D.; Cramer, C. J.; Truhlar, D. G. *J. Phys. Chem. B* **1998**, *102*, 3257.

(107) Marenich, A. V.; Olson, R. M.; Chamberlin, A. C.; Cramer, C. J.; Truhlar, D. G. *J. Chem. Theory Comput.* **2007**, *3*, 2055.

(108) Kelly, C. P.; Cramer, C. J.; Truhlar, D. G. *J. Phys. Chem. B* **2007**, *111*, 408.

(109) Kelly, C. P.; Cramer, C. J.; Truhlar, D. G. *J. Phys. Chem. A* **2006**, *110*, 2493.

(110) Kelly, C. P.; Cramer, C. J.; Truhlar, D. G. *J. Phys. Chem. B* **2006**, *110*, 16066.

(111) Lommerse, J. P. M.; Price, S. L.; Taylor, R. *J. Comput. Chem.* **1997**, *18*, 757. Misquitta, A. J.; Szalewicz, K. *J. Chem. Phys.* **2005**, *122*, 214109.

(112) Aidas, K.; Møgelhøj, A.; Kjaer, H.; Nielsen, C. B.; Mikkelsen, K. V. *J. Phys. Chem. A* **2007**, *111*, 4199.

(113) Cossi, M.; Crescenzi, O. *J. Chem. Phys.* **2003**, *118*, 8863.

CT900258F